TRANSIENT RESPONSE OF PIPELINES CARRYING HOMOGENEOUS COAL SLURRIES

By

VIJAY KUMAR MADDALI

Bachelor of Engineering
Andhra University
Waltair, India
1972

Master of Engineering
Indian Institute of Science
Bangalore, India
1974

Submitted to the Faculty of the
Graduate College of the
Oklahoma State University
in partial fulfillment of
the requirements of
the Degree of
DOCTOR OF PHILOSOPHY
December, 1979

TRANSIENT RESPONSE OF PIPELINES CARRYING

HOMOGENEOUS COAL SLURRIES

hesis Approved:

Karl N. Reid
Thesis Advisor

Jerald D. Parker

Lyman R. Ebbesen

Robert J. Mulholland

Norman N. Durham
Dean of the Graduate College

ACKNOWLEDGMENTS

Many persons have contributed in some way either directly or indirectly in this work. The author wishes to thank them all and would like to mention some of them by name.

Dr. Karl N. Reid, my advisor and the chairman of the advisory committee, has been instrumental in my choosing the problem. I am indebted to him for his invaluable guidance and encouragement througout this study and for his advice on the preparation of this thesis.

I am also thankful to my committee members, Dr. Lynn R. Ebbesen and Dr. Jerald D. Parker, with whom I had many fruitful discussions. I wish to thank Dr. Robert J. Mulholland of Electrical Engineering for serving on my committee.

Experimental work could not have been completed without the help of several individuals. My sincere thanks go to Dr. John A. Wiebelt, Dr. Earnest C. Fitch of Fluid Power Research Center, Dr. James V. Parcher of Civil Engineering, Mr. J. G. Montfort of Black Mesa Pipeline, Inc., Flagstaff, Arizona, Mr. Grant Young of AMOCO Research Center, Tulsa, Oklahoma, and Mr. George M. Cooper of Mechanical Engineering Laboratory.

I wish to thank all my friends and colleagues who were helpful in many ways in completing this work.

I acknowledge the financial support provided by the School of Mechanical and Aerospace Engineering, Oklahoma State University, in the form of teaching and research assistantships.

Special thanks are extended to Mrs. Susie Fuller for doing an excellent job in typing the manuscript, and to Mrs. Nita Brooks for drafting the figures.

Finally, I acknowledge with deep gratitude and dedicate my thesis to my father, Venkata Subbayya Maddali, who provided continuing encouragement and support throughout my academic endeavors.

TABLE OF CONTENTS

TABLE

LIST OF FIGURES

NOMENCLATURE

A	- Cross sectional area of the pipe normal to the z direction (in^2)
a	- Velocity of sound in the fluid (in/sec)
a_0	- Velocity of sound in the fluid at an operating point (in/sec)
CDL	- Discharge coefficient of valve orifice
c	- Ratio of yield stress to wall shear stress
c_v	- Volumetric concentration of solids to liquid
c_w	- Concentration of solids to liquid by weight
D	- Diameter of the pipe (in)
D/Dt	- Substantional derivative operator
e	- Base of the natural logarithm
exp	- Exponential function
f_i	- Functional relationship
f(t)	- Pressure gradient as a function of time (lbf/in^3)
f	- Friction factor
F	- Value of function f(t) at a given time t (lbf/in^3)
g	- Gravitational constant (in/sec^2)
$\vec{g}$	- Gravitational acceleration vector (in/sec^2)
g_r, g_θ, g_z	- Acceleration due to gravity in component direction (r, θ & z respectively) (in/sec^2)
K	- Constant used in characteristic equations
k	- Bulk viscosity ($lbf\ sec/in^2$)
L	- Length of the pipeline (in)

N_K - Normalized characteristic impedance of a transmission line

N_R - Reynolds number

N_r - Laminar resistance at reference conditions p_f/q_f (psi-sec/in^3)

n - Ratio of volume of air to liquid

P - Pressure (lbf/in^2)

p - Pressure (lbf/in^2)

p_f - Reference pressure (lbf/in^2)

p' - Normalized pressure (p/p_f)

p_e - Initial saturation pressure (lbf/in^2)

p_g - Gas pressure above the liquid at the beginning of evolution process (lbf/in^2)

p_{ca} - Pressure inside cavity (lbf/in^2)

p_0 - Atmospheric pressure (lbf/in^2)

q - Volumetric flow rate (in^3/sec)

q_f - Volumetric flow rate at reference condition (in^3/sec)

q' - Normalized volumetric flow rate (q/q_f)

$\vec{q}$ - Heat flux vector (lbf/in-sec)

R - Radius of pipeline (in)

r - Radial distance in cylindrical coordinate system (in)

s - Solubility constant

T_c - Time constant of evolution process (sec)

T_e - Half-life of evolution (sec)

t - Time (sec)

t_c - Characteristic time (L/a_0) (sec)

t' - Normalized time (t/t_c)

Δt - Time step (sec)

$\hat{U}$ - Internal energy per unit mass of the fluid (in^2/sec^2)

v - Velocity of the fluid (in/sec)

$\vec{v}$ - Velocity vector of the fluid (in/sec)

v_1, v_2 - Velocities at section 1 and section 2 (in/sec)

V_M - Maximum volume of air that can be released

V_ℓ - Volume of liquid evolving air (in^3)

V_e - Volume of air evolved at standard conditions (in^3)

V_f - Reference Volume ($Q_f t_c$) (in^3)

ΔV - Increment of the volume of air evolved (in^3)

$\bar{v}_z$ - Average velocity in z-direction (in/sec)

z - Axial distance in z-direction in the cylindrical coordinate system (in)

z_m - Zeros of the Bessel function $J_0(x)$

Δz - Distance between grids (in)

α - Fractional constant

β - Bulk modulus of the liquid (lbf/in^2)

β_e - Effective bulk modulus of the liquid (lbf/in^2)

δ - Increment in shear stress (lbf/in^2)

$\dot{\varepsilon}$ - Shear rate (sec^{-1})

λ - Dummy variable of convolution integral

μ, μ_0 - Viscosity ($lbf\ sec/in^2$)

η - Coefficient of plasticity ($lbf\ sec/in^2$)

ν - Ratio of viscosity or coefficient of plasticity to density of fluid (in^2/sec)

ρ - Density of the fluid ($lbf\ sec^2/in^4$)

ρ_0 - Density of the fluid at the operating condition ($lbf\ sec^2/in^4$)

$\vec{\vec{\tau}}$ - Shear stress tensor (lbf/in^2)

τ_{ij} - Shear stress acting along j perpendicular to the plane containing i (lbf/in^2)

τ_0 - Yield stress (lbf/in^2)

τ_w - Wall shear stress (lbf/in^2)

τ'_w - Normalized wall shear stress

$\hat{\phi}$ - Potential energy (in^2/ sec^2)

∇ - Del operator

CHAPTER I

INTRODUCTION

Coal has gained importance in recent years as an alternative source of energy to oil and gas. The transportation of coal also has become important. Railroads and waterways have been the most popular means of transportation of coal. However, as the demand for coal increases, faster and more economical ways of transportation are needed. One such way is the transportation of a coal-water slurry through a pipeline. There are already a few such pipelines in use; e.g. the Mesa coal pipeline between a coal mine site in the Navajo-Hopi Indian reservation in Arizona and the Mohave power plant in Nevada covers a distance of 273 miles. The growing interest in such pipelines can be evidenced by the plan of Energy Transportation Systems, Inc., of New Jersey to have a 38 inch diameter underground coal slurry pipeline from Campbell County, Wyoming, 1040 miles to the Middle South Utilities System's power generating complex in south-central Arkansas. Also, coal-water slurries themselves are involved as an in-plant process in coal gasification and liquification.

To make the transportation of coal in the form of slurries economical and safe, good design techniques are needed that take into account the severe pressure transients that can occur during startup and shutdown operations or due to unforeseen circumstances such as pump power failure, pipeline rupture, or sudden valve closure. Dynamic

models exist for pipelines carrying Newtonian fluids and these models are being used for better design of pipelines. Since coal-water slurries are non-Newtonian fluids the models developed for Newtonian fluids may not be applicable to coal slurry pipelines. For illustration, a pipeline of length 2941 in. and internal diameter of 1 in. has been simulated on a digital computer using two dynamic models. The first model is based on the non-Newtonian nature of coal slurry and the other model treats the coal slurry as a Newtonian fluid with an apparent viscosity. The results of the simulation of these two models for a sudden valve closure at the downstream end of the line are shown in Figure 1. The computed results in Figure 1 indicate that the attenuation characteristic of a coal slurry pipeline is predicted differently by the two models. A comparison of these two models with experimental results in Chapter VI shows that a model which accounts for the non-Newtonian nature of a coal slurry is more appropriate for predicting the pressure transients in a pipeline.

Dynamic models that consider the non-Newtonian behavior of coal slurries can be very useful in the optimum design of the pipelines, e.g. selection of wall thicknesses, pipe material, valve closure times, etc.. Also, increasing use is being made of computers to monitor and control slurry flows through pipelines. Appropriate dynamic models are needed in such cases for controller design and implementation.

An important consideration in pipeline design is whether or not cavitation bubbles form (i.e., the "column separates") at certain points along the pipeline. Presence of cavitation creates very low pressures inside the pipeline. When transient forces acting within a pipeline cause a cavitation bubble to collapse, the local pressure may rise

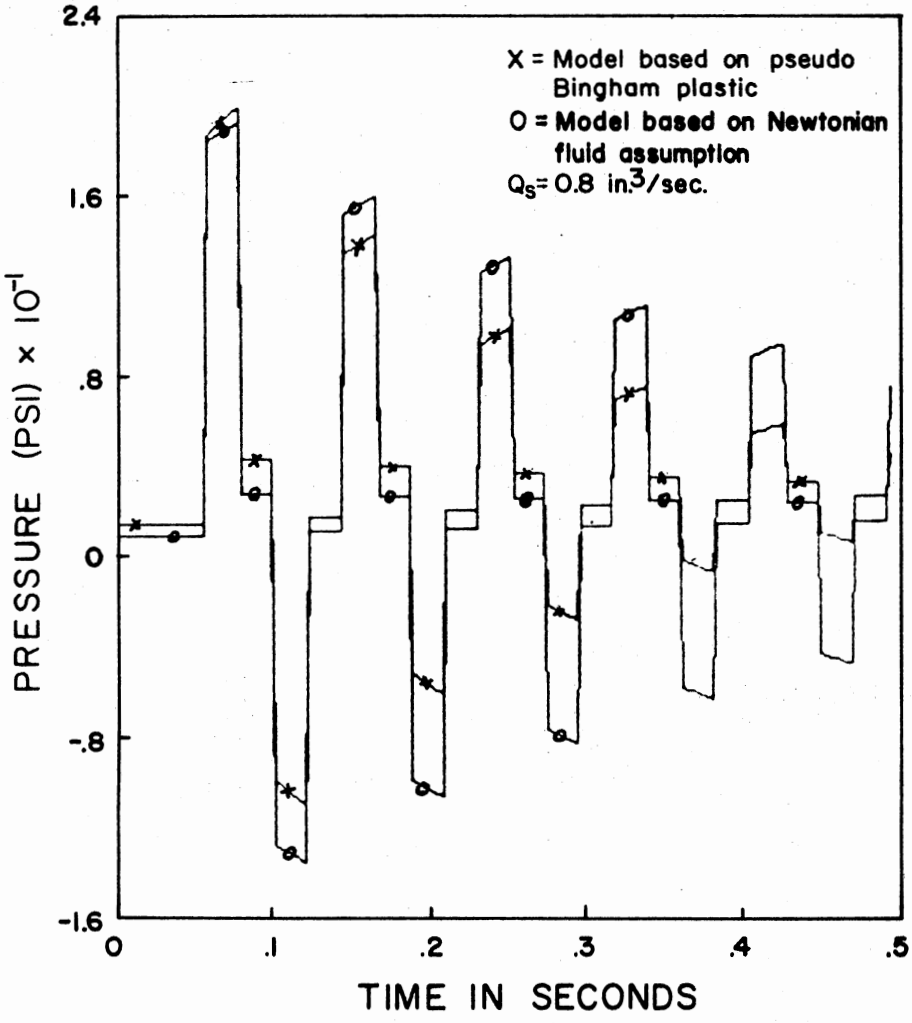

Figure 1. Comparison Between Two Models

suddenly to a very high value. Sudden pressure variations from below atmospheric to several orders of magnitude above atmospheric pressure subject the pipewall to severe transient stresses. Due to the presence of solid particles in a coal slurry, severe erosion may accompany cavitation bubble formation and collapse. Research is underway to predict the occurrence of cavitation and resulting column separation more accurately in a pipeline. As yet, a generalized model has not been obtained. However, even a simple model that can be used to predict cavitation and the resulting column separation fairly accurately for a particular fluid like a coal slurry would enhance pipeline design. Such a dynamic model would aid the design of surge pressure suppression devices and the selection of safe valve closure times. The research described in this dissertation was motivated by the needs described above for a dynamic model for pipelines carrying coal slurries.

Rheological Characteristics of a Coal Slurry

The coal slurries that are currently being used have different compositions consisting of various sizes and concentrations of coal particles. However, the slurries that are being used in long distance transportation generally have relatively small sized particles in high concentrations so as to have very low settling velocities and high packing density. The shear stress/shear rate relations for these fluids are non-Newtonian in character. Non-Newtonian fluids are broadly classified as pseudoplastic, dilatant or Bingham plastic (see Figure 2). Fluids can also be classified according to the time-dependent nature of the shear stress for a given shear rate. If shear stress decreases with respect to time, then the fluid is called

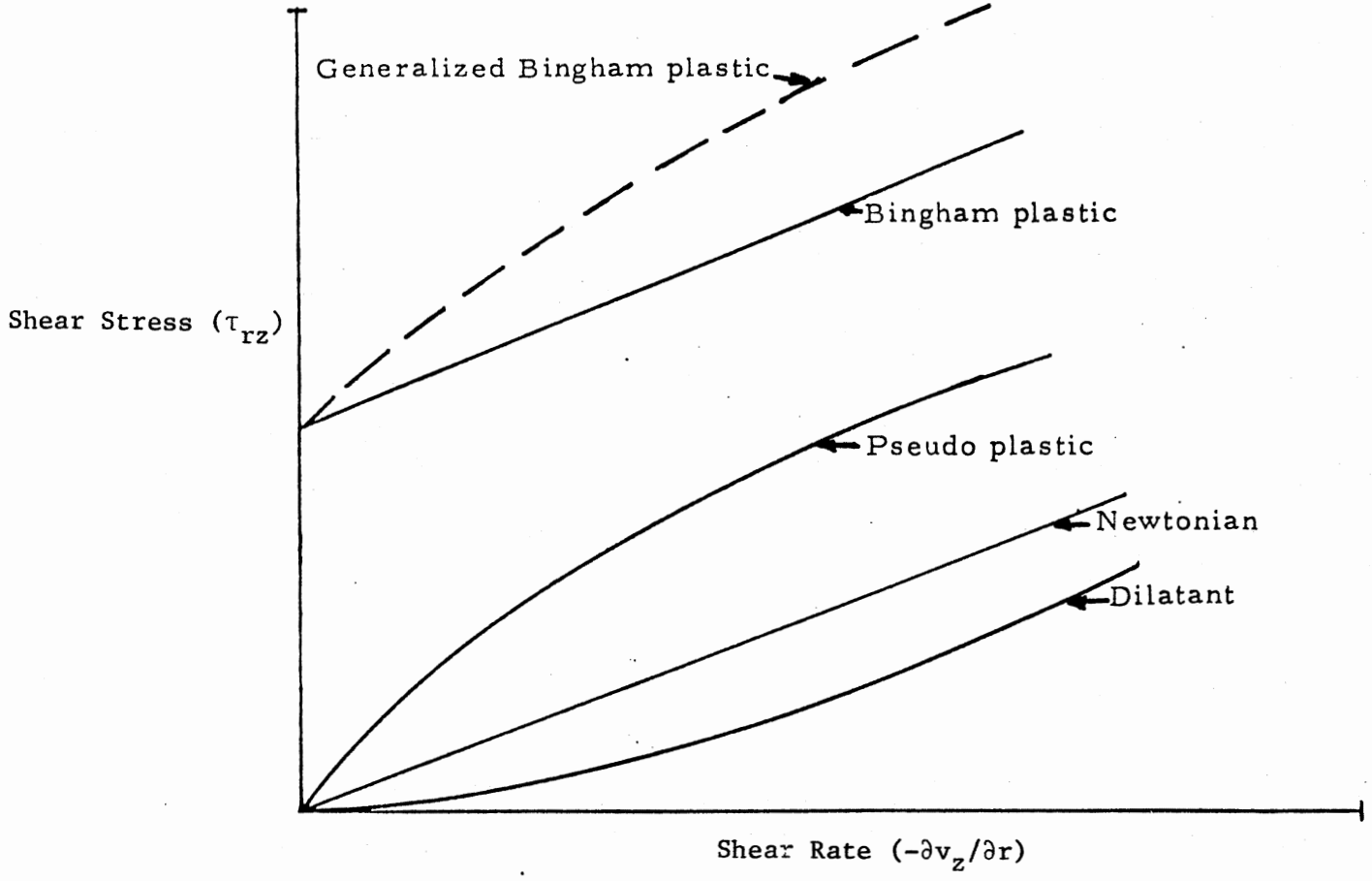

Figure 2. Classification of Basic Fluid Types in Terms of Shear Stress/Shear Rate Relations.

thixotropic. If it increases, the fluid is rheopectic. For high concentrations and small particle sizes of coal, a coal slurry behaves approximately like a homogeneous thixotropic Bingham plastic fluid [1], even though the behavior at small shear rates is Newtonian.

Based on the available literature, it is believed that the most simple and appropriate rheological model for a coal slurry involving high concentrations of fine coal particles is the pseudo-Bingham plastic model illustrated in Figure 3. The pseudo-Bingham plastic model can be characterized as follows:

$$\tau_{rz} = \tau_0 + \eta \left(-\frac{\partial v_z}{\partial r}\right) \quad \text{for} \quad \tau_{rz} \geq \tau_0 + \delta \tag{1.1}$$

$$\tau_{rz} = \mu_0 \left(-\frac{\partial v_z}{\partial r}\right) \quad \text{for} \quad \tau_{rz} \leq \tau_0 + \delta \tag{1.2}$$

where δ is a small increment in shear stress. As δ tends to zero, τ_{rz} tends to τ_0 at $\partial v_z/\partial r = 0$. In other words, the rheological behavior of a pseudo-Bingham plastic fluid approaches that of an ideal Bingham plastic fluid as δ tends to zero.

Objectives and Scope of Study

The primary objectives of the study were the following:

1. To extend the one-dimensional constant friction dynamic model for pipelines carrying Newtonian fluids [2] to pipelines carrying coal slurries or pseudo-Bingham plastic fluids. Column separation effects and operation of the line in both laminar and turbulent flow regimes should be considered. The constant friction dynamic model for the turbulent flow regime would be based on experimental results for slurry flow in the turbulent flow regime [4].

2. To develop a one-dimensional time-dependent friction

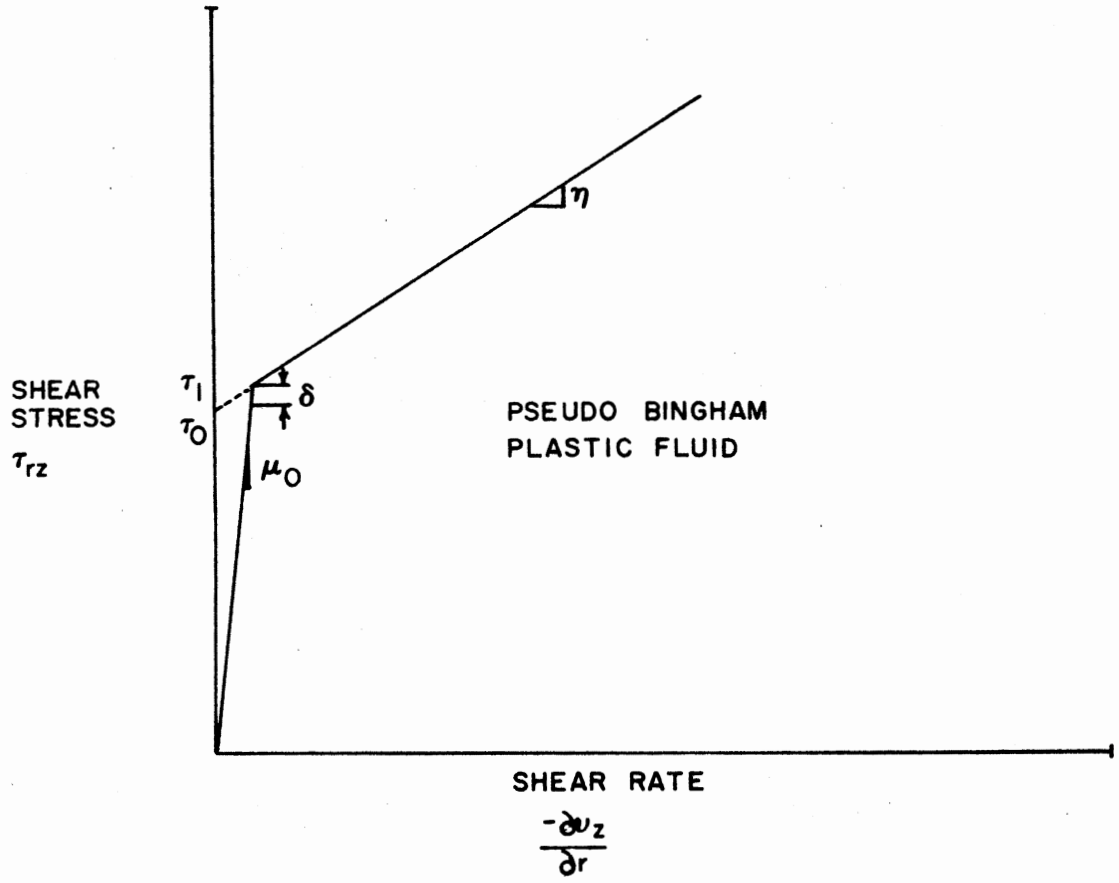

Figure 3. Rheogram for Pseudo Bingham Plastic Fluid.

dynamic model for unsteady laminar flow in a coal slurry pipeline. This model is similar to but not a simple extension of the time-dependent friction model for Newtonian fluids [3].

3. To validate the constant friction and time-dependent friction models through experiments with a coal slurry that has a rheological characteristic that can be approximated by the pseudo-Bingham plastic fluid model. The constant friction model also should be validated when there is column separation in the line.

Plan of Presentation

A summary of the literature reviewed for this study is presented in Chapter II. Basic water hammer equations are developed in Chapter III. Chapter IV covers the modelling procedures for the constant friction and the time-dependent friction models in the laminar flow regime. An algorithm that extends the constant friction model to the turbulent flow regime is also presented in Chapter IV. Details of all derivations are given in Appendix A. A simple cavity growth model is developed in Chapter V along with an algorithm to include the cavitation model in the constant friction line model to predict column separation in a pipeline. Validation of the various models with experiments is discussed in Chapter VI. The conclusions and recommendations appear in Chapter VII. Program listings for all computer programs used are presented in Appendix B.

CHAPTER II

LITERATURE SURVEY

A summary of related literature is presented in this chapter. Though the dissertation is primarily related to dynamic models for coal slurry, the literature survey included other types of slurries and liquids that behave like Bingham plastic fluids or pseudo-Bingham plastic fluids. The survey indicated the following:

1. No attempt has been made to study the general transient behavior of Bingham plastic fluids in a pipeline subjected to sudden changes in input or boundary conditions, although unsteady flow behavior of Bingham plastic fluids at a cross-section of a pipeline subjected to step input pressure gradient has been studied using analytical or numerical methods. In the case of pseudo-Bingham plastic fluids, no literature is available regarding unsteady flow.

2. Experimental data on the unsteady flow of Bingham plastic fluids or pseudo-Bingham plastic fluids such as coal slurry is not available.

Since the flow behavior of coal slurries is of primary importance to this dissertation a brief review of literature on coal slurries is given. This review is followed by a survey of the literature on Bingham plastic fluids, unsteady flow of Newtonian fluids (as is relevant for the current study) and column separation effects in pipelines.

Behavior of Coal and Charcoal Slurries

There is considerable literature on the behavior of coal slurries.

Though coal slurries are basically two-phase fluids, they have been treated as homogeneous single-phase fluids under certain conditions. These conditions are when the coal slurry has a very low settling velocity[1], and when the relative velocity between the particles and the liquid is very small. Under these conditions the coal slurry behaves like single-phase non-Newtonian liquid. The coal slurry composition that is being used currently to transport coal over long distances through pipelines generally consists of small particle sizes of coal in high concentrations mixed with water. Faddick [1] showed that a coal slurry with such a composition behaves like a non-Newtonian fluid and at sufficiently high concentrations it behaves like a Bingham plastic fluid. From the rheogram presented in Reference [1] and which is reproduced in Figure 4, coal with a mean size of 2200 microns mixed with water in high concentrations appears to behave approximately as a pseudo-Bingham plastic fluid. In another study, Sacks, Romney, Jones [5] presented data related to charcoal slurry flow through pipelines. They correlated the pipeline data with the steady-state analytical model developed by Buckingham and Reiner [6,7,8]. From their results, charcoal slurries behave like Bingham plastic fluids at concentrations greater than 40% by weight and for small particle sizes[2]. Similar results have been reported by Bain and Bonnington [9].

---

[1]Small particles have a tendency to settle only at extremely low liquid velocities.

[2]Less than 325 mesh.

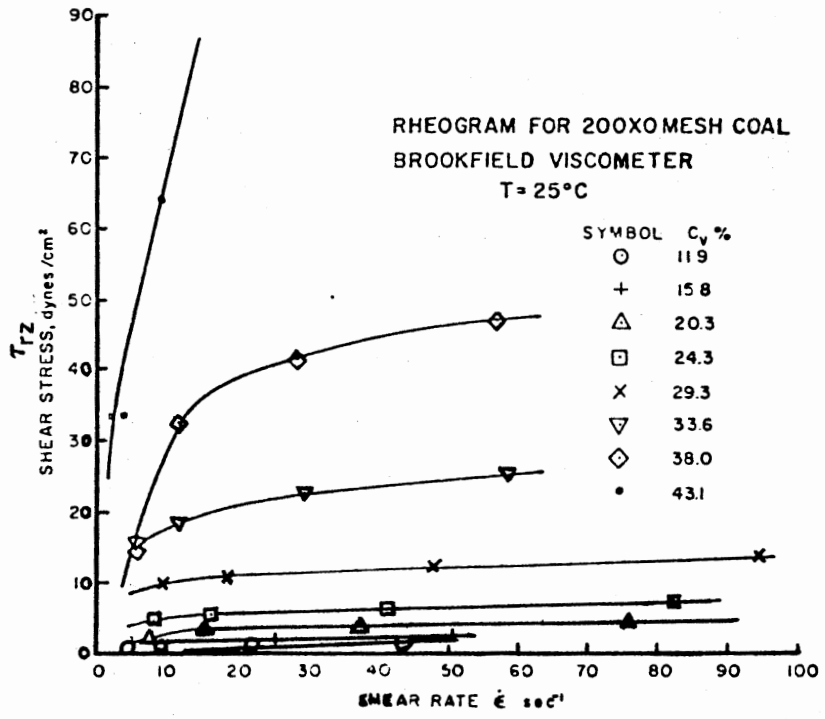

Figure 4. Rheogram for 100x0 Mesh Coal

Bingham Plastic Fluids

Steady Flow of Bingham Plastic Fluids

Bingham and Green in 1919 suggested a two parameter model for the shear stress/shear rate relationship for fluids like paints, pastes, and suspensions. Later Buckingham and Reiner [6,7,8] obtained the steady-state analytical relationship between flow rate and pressure drop for the laminar flow of a Bingham plastic fluid in a circular line. The Buckingham-Reiner equation has been found to describe adequately the flow through a capillary tube for a wide range of shear rates by researchers like Caldwell and Babbit [10], McMillen [11], and Thomas [12]. Steady-state models have also been developed for Bingham plastic fluids in the turbulent flow regime. These models are empirical in nature, like the corresponding ones for turbulent flow of Newtonian fluids in pipelines. A good description of the literature on non-Newtonian fluids, including their behavior in the turbulent flow regime under steady-state conditions, can be found in books by Wilkinson [13], Skelland [14]. Among the steady-state friction models for the turbulent flow regime, the most convenient one is the model developed by Tomita [4] for Bingham plastic fluids like slurries, muds, etc. Tomita's model is discussed in detail in a later chapter. Much work has also been done in determining the two parameters τ_0 and η for various fluids like pastes, paints and slurries [15] which have been treated as Bingham plastic fluids. However, very little mention is made of coal slurries in the above references, viz. [13,14,15].

Based on the work of Faddick [1], Sacks et al. [5], Bain and Bonnington [9], it is believed that a pseudo-Bingham plastic model is

appropriate for describing the rheological characteristics of coal slurries with high concentrations of small particles. The rheograms obtained for the coal slurry used in the experiment show that the fluid rheological behavior resembles more that of a pseudo-Bingham plastic fluid than an ideal Bingham plastic fluid.

Unsteady Flow of Bingham Plastic Fluids

In contrast to the extensive studies conducted on the steady flow of Bingham plastic fluids, limited work has been done on the unsteady flow of Bingham plastic fluids in circular cross-section lines. Atabek [16] derived expressions for the velocity profiles during the start-up flow of a Bingham plastic fluid in a circular line. However this analysis is based on the assumption that the line is long enough that there are no pressure wave reflections. Duggins [17] solved the same problem numerically using finite element methods and claimed that his solution is more accurate than the analytical solution given by Atabek [16]. Duggin's solution technique eliminated the discontinuity in the acceleration and the stress gradient that appears across the boundary of the core and sheared annulus in Atabek's solution. Beaman [18] also obtained independently similar numerical solutions for the transient velocity profiles of Bingham plastic fluids for a step pressure gradient along the line. His treatment of the problem was similar to that of Meyer [19] who obtained a numerical solution for a two-phase heat conduction problem using the well known "Method of Lines" technique[3].

[3]Beaman did not reference the earlier work of Atabek and Duggins.

Unsteady Flow of Newtonian Fluids

There is a vast amount of literature regarding the unsteady flow of Newtonian fluids. Some of the related references are given in the bibliography [2,3,20,21,22,23]. The most comprehensive time-domain model for unsteady flow of a Newtonian fluid in the laminar flow regime is the time-dependent friction model developed by Zielke [3] and improved by Brown [23] using the Method of Characteristics. This model is valid for small amplitude signals with negligible through flow. In the current dissertation, a model that is similar to the one developed by Zielke for Newtonian fluids is formulated for pipelines carrying coal slurries that behave like a pseudo-Bingham plastic fluid. Another model that is less comprehensive but is computationally faster is the constant friction model [2]. The constant friction model also uses the Method of Characteristics solution technique. A similar model has been developed by the author and is described in a later chapter.

Column Separation

Column separation is a phenomenon where a cavity is formed between two columns of liquid. It has been assumed that whenever the pressure at any point in the line falls below the vapor pressure of the liquid, cavitation occurs. A review of models used for cavitation in pipelines can be found in the textbook by Wylie and Streeter [2]. A few references relevant to present dissertation are discussed. Some investigators have assumed that once the pressure at a point in a pipeline reaches the fluid vapor pressure, the fluid vaporizes and the minimum pressure is always the vapor pressure. Baltzer [24] and Streeter [25] used this

vapor pressure assumption in predicting the pressure transients in a pipeline in which column separation occurred. Safwat and Van der Polder [26] attempted to validate this vapor pressure assumption by studying experimentally a pipeline terminated by a shut-off valve and carrying pure water. In their experiments column separation was caused to occur downstream of the valve by suddenly closing the valve. Though the first peak pressure immediately after cavitation matched in amplitude with analytical predictions, the latter peaks did not match either in amplitude or with the time of occurrence of the peaks.

Scweitzer and Szebehely [27] found that cavitation often is associated with the release of dissolved air rather than simply liquid vaporization. Driels [28] used this concept of air release to model the behavior of a cavity which often forms in a liquid line just downstream of a closing valve. Driels also obtained good experimental correlation for the first peak and a better correlation for the second peak than others did with their models using the vapor only mechanism. Kerosene, which contains a large amount of air, was used as the liquid medium in Driels' experiments. Air was released only at the downstream end of the valve. Scweitzer and Szebehely [27] also found that the percentage of dissolved air is very small in certain liquids like pure water, and that the cavity bubble is predominantly occupied by liquid vapor rather than air (gas). In an analytical study, Brown [29] allowed air release to occur at certain points along the pipeline and treated the released air as discrete pockets. For slow transients such as the pump failure cases reported by Brown, the results are satisfactory as far as the peak amplitude predictions are concerned. For rapid transients such as sudden valve closures, Brown's method of releasing air led to

instability in the solution. The cavitation models discussed so far are based on macroscopic analysis of the air bubble. Another type of cavitation model takes into account the microscopic behavior of individual bubbles [30]. Though by far this approach seems to result in better correlations with experiments, it seems to have one serious drawback. That is, it is difficult to estimate apriori the number of bubbles in a given fluid volume and experiments have to be performed to get an estimate. This estimate may or may not be close to the actual number of bubbles that may exist for a given pipeline system. For rapid transients and with low air content, the solutions using the microscopic approach also are not stable numerically and various artificial means are necessary to stabilize the solutions.

CHAPTER III

BASIC EQUATIONS OF WATER HAMMER FOR PSEUDO BINGHAM PLASTIC FLUIDS

Basic equations for a fluid transmission line with a Newtonian fluid have been presented by several authors. The equations for a transmission line with a pseudo-Bingham plastic fluid are essentially the same except for the friction term. Though the following equations have been obtained earlier by others, they are repeated here for the sake of completeness.

In vectorial form, the following are the equations that describe the flow of fluid [31]:

Continuity:

$$\frac{\partial \rho}{\partial t} + \nabla \cdot (\rho \vec{v}) = 0 \tag{3.1}$$

Equation of Motion:

$$\rho \left(\frac{\partial \vec{v}}{\partial t} + (\vec{v} \cdot \nabla)\vec{v}\right) = -\nabla p - \nabla \cdot \vec{\vec{\tau}} + \rho \vec{g} \tag{3.2}$$

Energy:

$$\rho \frac{D}{Dt} \left(\hat{U} + \hat{\phi} + \frac{1}{2} v^2\right) = -(\nabla \cdot \vec{q}) - (\nabla \cdot p\vec{v}) - (\nabla \cdot [\vec{\vec{\tau}} \cdot \vec{v}]) \tag{3.3}$$

The above equations are based on the assumption that the fluid is homogeneous. No other additional assumptions are made.

The energy equation is not considered hereafter as it is assumed that the temperature variations along the pipeline are negligible and the rates of change of fluid properties are small compared to the rates of change of the other variables.

Equation (3.2) when expanded into the r,θ,z components of a cylindrical co-ordinate system will result in three scalar equations [31]. These equations can be simplified further by using the following assumptions:

a) $v_r = 0$, $v_\theta = 0$.

b) Flow is axi-symmetric.

c) $g_r = 0$, $g_\theta = 0$.

The resulting equations are as follows:

Continuity:

$$\frac{\partial \rho}{\partial t} + \frac{\partial}{\partial z} (\rho v_z) = 0 \tag{3.4}$$

r-Momentum:

$$0 = - \frac{\partial p}{\partial r} - \left(\frac{1}{r} \frac{\partial}{\partial r} (r \tau_{rr}) - \frac{\tau_{\theta\theta}}{r} + \frac{\partial \tau_{rz}}{\partial z}\right) \tag{3.5}$$

θ-Momentum:

$$0 = -\left(\frac{1}{r^2} \frac{\partial}{\partial r} (r^2 \tau_{r\theta}) + \frac{\partial \tau_{\theta z}}{\partial z}\right) \tag{3.6}$$

z-Momentum:

$$\rho \left(\frac{\partial v_z}{\partial t} + v_z \frac{\partial v_z}{\partial z}\right) = - \frac{\partial p}{\partial z} - \left(\frac{1}{r} \frac{\partial}{\partial r} (r \tau_{rz}) + \frac{\partial \tau_{zz}}{\partial z}\right) + \rho g_z \tag{3.7}$$

In the case of Newtonian fluids, the stress tensor components are functions of v_r, v_θ, v_z, μ, k as given below:

$$\tau_{rr} = f_1(v_r, v_\theta, \frac{\partial v_z}{\partial z}, \mu, k) \tag{3.8}$$

$$\tau_{rz} = f_2(\frac{\partial v_z}{\partial r}, v_r, \mu) \tag{3.9}$$

$$\tau_{\theta\theta} = f_3(v_\theta, v_r, \frac{\partial v_z}{\partial z}, \mu, k) \tag{3.10}$$

$$\tau_{r\theta} = f_4(v_\theta, v_r, \mu) \tag{3.11}$$

$$\tau_{\theta z} = f_5(v_\theta, \frac{\partial v_z}{\partial \theta}, \mu) \tag{3.12}$$

$$\tau_{zz} = f_6(\frac{\partial v_z}{\partial z}, v_r, v_\theta, \mu, k) \tag{3.13}$$

Exact functional relationships are presented in reference 31. The above equations are based on the rheological relationship of Newtonian fluids which is as follows:

$$\tau = \mu \dot{\varepsilon}. \tag{3.14}$$

In the case of the pseudo-Bingham plastic fluids, the relationship between shear stress and strain rate is as follows:

$$\tau = \tau_0 + \eta\dot{\varepsilon} \quad \text{for} \quad \tau \geq \tau_0 + \delta \tag{3.15}$$

and

$$\tau = \mu_0\dot{\varepsilon} \quad \text{for} \quad \tau \leq \tau_0 + \delta. \tag{3.16}$$

The functional relationships of the stress tensor components are similar to those of Newtonian fluids except for the additional parameter τ_0.

Hence Equation (3.5) reduces to the following equation for Newtonian as well as pseudo-Bingham plastic fluids.

r-Momentum:

$$0 = -\frac{\partial p}{\partial r} - \frac{\partial \tau_{rr}}{\partial r} - \frac{\partial \tau_{rz}}{\partial z} \tag{3.17}$$

The right-hand side of Equation (3.6) reduces to zero.

Assuming that axial gradients of velocity and temperature can be neglected with respect to the radial gradients, and that the variation of the axial velocity gradient in the radial direction can be considered to be small, it can be deduced from Equation (3.17) that pressure is constant along the radial direction. In addition, the z-momentum equation reduces to the following:

z-Momentum:

$$\rho\left(\frac{\partial v_z}{\partial t} + v_z\frac{\partial v_z}{\partial z}\right) = -\frac{\partial p}{\partial z} - \frac{1}{r}\frac{\partial}{\partial r}(r\,\tau_{rz}) + \rho g_z. \tag{3.18}$$

Equations (3.4) and (3.18) describe the flow of Newtonian or pseudo-

Bingham plastic fluids in a circular pipeline under isothermal conditions.

Since there are four unknowns i.e. v_z, p, ρ, τ_{rz}, two more equations are needed. They are the following:

Equation of State:

$$dp = \beta \frac{d\rho}{\rho_0} \tag{3.19}$$

Rheological Relationship:

$$\tau_{rz} = \tau_0 + \eta(-\frac{\partial v_z}{\partial r}) \quad \text{for} \quad \tau_{rz} \geq \tau_1 \tag{3.20}$$

$$\tau_{rz} = \mu_0 (-\frac{\partial v_z}{\partial r}) \quad \text{for} \quad \tau_{rz} \leq \tau_1 \tag{3.21}$$

where $\tau_1 = \tau_0 + \delta$.

Rewriting Equation (3.4) after substituting Equation (3.19) for ρ in (3.4) and assuming small variations in density, gives

$$\frac{1}{\beta}\frac{\partial p}{\partial t} + \frac{\partial v_z}{\partial z} + \frac{v_z}{\beta}\frac{\partial p}{\partial z} = 0. \tag{3.22}$$

Equations (3.22), (3.18), (3.20), and (3.21) are used in later chapters to describe the flow of a pseudo-Bingham plastic fluid in a circular pipeline under constant temperature conditions.

CHAPTER IV

WALL SHEAR STRESS EVALUATION FOR UNSTEADY FLOW

The basic equations to be solved for unsteady pseudo-Bingham plastic fluid flow through a constant diameter pipeline have been given in the previous chapter. Similar equations already exist for Newtonian fluids. In this chapter the basic equations derived in the previous chapter will be averaged to make the equations one-dimensional. Then, evaluation of the wall shear stress using steady-state friction and time-dependent friction will be discussed. Calculation of steady-state friction and time-dependent friction will be based on the fact that coal slurry behaves like a pseudo-Bingham plastic fluid.

Equations (3.22) and (3.18) are the same for Newtonian fluids also. The difference lies in the rheological relationships for Newtonian and pseudo-Bingham plastic fluids. If R is the radius of a pipeline, integrating continuity and z-momentum equations with respect to r and dividing by the area of cross-section A, gives:

Continuity:

$$\frac{2\pi}{\beta A}\int_0^R \left(\frac{\partial p}{\partial t}\right) r\,dr + \frac{2\pi}{\beta A}\int_0^R \left(v_z \frac{\partial p}{\partial z}\right) r\,dr + \frac{2\pi}{A}\int_0^R \left(\frac{\partial v_z}{\partial z}\right) r\,dr = 0 \qquad (4.1)$$

z-Momentum:

$$\frac{2\pi\rho_0}{A}\int_0^R \left(\frac{\partial v_z}{\partial t} + v_z\frac{\partial v_z}{\partial z}\right) rdr = -\frac{2\pi}{A}\int_0^R \left(\frac{\partial p}{\partial z}\right) rdr$$

$$-\frac{2\pi}{A}\int_0^R \left(\frac{1}{r}\frac{\partial}{\partial r}(r\tau_{rz})\right) rdr + \frac{2\pi\rho_0}{A}\int_0^R g_z\, rdr. \qquad (4.2)$$

The convective acceleration term $v_z\frac{\partial v_z}{\partial z}$ is small compared to the local acceleration $\frac{\partial v_z}{\partial t}$. So $\frac{2\pi}{A}\int_0^R \left(v_z\frac{\partial v_z}{\partial z}\right) rdr$ can be approximated as $\bar{v}_z\frac{\partial \bar{v}_z}{\partial z}$. Also pressure does not vary across the cross-section. Equations (4.1) and (4.2) will then reduce to the following in terms of q. The gravitational force term is included in the pressure force term.

Continuity:

$$\frac{1}{\beta}\frac{\partial p_t}{\partial t} + \frac{\bar{v}_z}{\beta}\frac{\partial p_t}{\partial z} + \frac{1}{A}\frac{\partial q}{\partial z} + \frac{\bar{v}_z}{\beta}\rho_0 g_z = 0 \qquad (4.3)$$

z-Momentum:

$$\frac{\rho_0}{A}\left(\frac{\partial q}{\partial t} + \bar{v}_z\frac{\partial q}{\partial z}\right) = -\frac{\partial p_t}{\partial z} - \frac{2\pi R}{A}\tau_w \qquad (4.4)$$

where $p_t = p - \rho_0 g_z z$.

Equations (4.3) and (4.4) coupled with the rheological relationship and the initial and boundary conditions can be used for determining the pressure and flow rate at any point along a pipeline. The method of characteristics' solution technique [32] can be used to solve the partial differential equations given above. This solution technique makes it possible to convert the hyperbolic partial differential

equations into ordinary differential equations along the characteristic lines.

Multiplying Equation (4.3) by a constant K and adding it to Equation (4.4), gives:

$$\frac{K}{\beta}\left(\frac{\partial p_t}{\partial t} + \left(\bar{v}_z + \frac{\beta}{K}\right)\frac{\partial p_t}{\partial z}\right) + \frac{\rho_0}{A}\left(\frac{\partial q}{\partial t} + \left(\frac{K}{\rho_0} + \bar{v}_z\right)\frac{\partial q}{\partial z}\right)$$

$$= -\frac{2\pi}{A} R\, \tau_w - \frac{K\bar{v}_z}{\beta}\rho_0 g_z \qquad (4.5)$$

Constant K should be so chosen that partial derivatives become total derivatives.

Since

$$\frac{dp}{dt} = \frac{\partial p}{\partial t} + \frac{\partial p}{\partial z}\frac{dz}{dt} \qquad (4.6)$$

then

$$\bar{v}_z + \frac{\beta}{K} = \frac{K}{\rho_0} + \bar{v}_z = \frac{dz}{dt} \qquad (4.7)$$

where $K = \pm\sqrt{\beta\rho_0}$. The velocity of sound in a liquid is given by $a = \sqrt{\beta/\rho}$.

Equation (4.5) then becomes after rearranging,

$$\frac{dp_t}{dt} + \left(\frac{\rho_0 a_0}{A}\right)\frac{dq}{dt} = -\frac{2\pi R}{A} a_0\, \tau_w - \bar{v}_z\, \rho_0 g_z \qquad (4.8)$$

when $\frac{dz}{dt} = \bar{v}_z + a_0$

and

$$-\frac{dp_t}{dt} + \left(\frac{\rho_0 a_0}{A}\right)\frac{dq}{dt} = -\frac{2\pi R}{A}\, a_0\, \tau_w + \bar{v}_z \rho_0 g_z \tag{4.9}$$

when $\frac{dz}{dt} = \bar{v}_z - a_0$.

Normalizing equations (4.8) and (4.9), yields

$$\frac{dp'}{dt'} + \left(\frac{\rho_0 a_0}{A}\right)\frac{1}{N_r}\frac{dq'}{dt'} = -\frac{2\pi RL}{A}\,\tau_w' - \frac{\bar{v}_z}{a_0}\,\rho_0\,\frac{g_z}{p_f}\,L \tag{4.10}$$

when $\frac{dz'}{dt'} = \frac{\bar{v}_z}{a_0} + 1$

and

$$-\frac{dp'}{dt'} + \left(\frac{\rho_0 a_0}{A}\right)\frac{1}{N_r}\frac{dq'}{dt'} = -\frac{2\pi RL}{A}\,\tau_w' + \frac{\bar{v}_z}{a_0}\,\rho_0\,\frac{g_z}{p_f}\,L \tag{4.11}$$

when $\frac{dz'}{dt'} = \frac{\bar{v}_z}{a_0} - 1$.

If $N_K = \left(\frac{\rho_0 a_0}{A}\right)\frac{1}{N_r}$,

then

$$\frac{dp'}{dt'} + N_K\frac{dq'}{dt'} = -4\left(\frac{L}{D}\right)\tau_w' - \bar{v}_z'\,\frac{\rho_0 g_z L}{p_f} \tag{4.12}$$

when $\frac{dz'}{dt'} = \bar{v}_z' + 1$

and

$$-\frac{dp'}{dt'} + N_K\frac{dq'}{dt'} = -4\left(\frac{L}{D}\right)\tau_w' + \bar{v}_z'\,\frac{\rho_0 g_z L}{p_f} \tag{4.13}$$

when $\frac{dz'}{dt'} = \bar{v}_z' - 1$.

Equations (4.12) and (4.13) can be solved on a digital computer using finite differences. To solve these equations, wall shear stress needs to be specified along with initial and boundary conditions. In the case of Newtonian fluids, the wall shear stress has been evaluated using either steady-state or time-dependent friction [2,3]. When using steady-state friction, the wall shear stress is a function of flow rate at a given instant of time. When time-dependent friction is used, it is not only a function of flow rate at a given instant of time but also a function of the past history of the velocity gradients. A similar approach can be used for evaluating the wall shear stress for a pseudo-Bingham plastic fluid such as coal slurry. Faddick [1] has obtained rheograms for coal slurries having different concentrations for a nominal particle size of 2200 microns (Figure 4). At high concentrations and with small particle sizes of coal, the rheological property of coal slurry is similar to that of a pseudo-Bingham plastic fluid (Figure 3).

If β_e, ρ_e are the effective bulk modulus and density respectively of a pseudo-Bingham plastic fluid, then the characteristic Equations (4.12) and (4.13) will still hold and the only difference will be in the evaluation of wall shear stress τ_w. If it is assumed that the maximum average velocity in the pipeline is considerably smaller than the velocity of sound and the elevation angle of the pipeline is small, then Equations (4.12) and (4.13) will simplify to the following equations:

$$\frac{dp'}{dt'} + N_{Ke} \frac{dq'}{dt'} = -4\left(\frac{L}{D}\right) \tau_w' \tag{4.14}$$

when $\frac{dz'}{dt'} = +1$

and

$$- \frac{dp'}{dt'} + N_{Ke} \frac{dq'}{dt'} = -4\left(\frac{L}{D}\right) \tau_w' \tag{4.15}$$

when $\frac{dz'}{dt'} = -1$.

Constant Friction Model

For a Bingham plastic fluid the rheological relationship at the wall is given by the following:

$$\tau_w = \tau_0 + \eta\left(- \frac{\partial v_z}{\partial r}\right)\Big|_{r=R} \quad \text{for} \quad \tau_w \geq \tau_0 \tag{4.16}$$

$$\frac{\partial v_z}{\partial r}\Big|_{r=R} = 0 \quad \text{for} \quad \tau_w \leq \tau_0. \tag{4.17}$$

The rheological behavior of a pseudo-Bingham plastic fluid can be modelled as follows:

$$\tau_w = \tau_0 + \eta\left(- \frac{\partial v_z}{\partial r}\right)\Big|_{r=R} \quad \text{for} \quad \tau_w \geq \tau_0 + \delta \tag{4.18}$$

$$\tau_w = \tau_0\left(- \frac{\partial v_z}{\partial r}\right)\Big|_{r=R} \quad \text{for} \quad \tau_w \leq \tau_0 + \delta. \tag{4.19}$$

The steady-state relationship between the wall shear stress and the flow rate of a pseudo-Bingham plastic fluid viz. coal slurry can be approximated by steady-state relationships for wall shear stress [31] of Newtonian and Bingham plastic fluids.

Treating the fluid as a Newtonian fluid for $\tau_w \leq \tau_0 + \delta$, then

$$\tau_w = \left(-\frac{\partial p}{\partial z}\right) \frac{R}{z} = \frac{4\mu_0 q}{\pi R^3} \tag{4.20}$$

in steady-state. Treating the fluid as a Bingham plastic fluid for $\tau_w \geq \tau_0 + \delta$,

$$q = \frac{\pi R^3}{4\eta} \tau_w - \frac{\pi R^3}{3\eta} \tau_0 + \frac{\pi R^3}{12\eta} \frac{\tau_0^4}{\tau_w^3} \quad \text{for} \quad \tau_w \geq \tau_0 + \delta. \tag{4.21}$$

Let $\tau_1 = \tau_0 + \delta$. When $\tau_w = \tau_1$,

$$q_1 = \frac{\pi R^3}{4\mu_0} \tau_1. \tag{4.22}$$

Knowing τ_0 and η from measured rheological characteristics, μ_0 is given by

$$\mu_0 = \frac{\eta}{1 - \frac{4}{3}\frac{\tau_0}{\tau_1} + \frac{1}{3}\left(\frac{\tau_0}{\tau_1}\right)^4}. \tag{4.23}$$

An explicit solution for τ_w in terms of q is quite involved in the case of Bingham plastic fluids. But Equation (4.21) can be recursively used to obtain the wall shear stress τ_w for a given q. This approach gives only an approximate wall shear stress of a pseudo-Bingham plastic fluid flowing in a pipeline. Normalizing Equations (4.20) and (4.21), yields

$$q' = \frac{4L}{D}\left(\tau_w' - \frac{4}{3}\tau_0' + \frac{1}{3}\tau_0'\left(\frac{\tau_0'}{\tau_w'}\right)^3\right) \quad \text{for} \quad q' \geq q_1' \tag{4.24}$$

$$\tau_w' = \frac{1}{4}\left(\frac{\mu_0}{\eta}\right)\frac{D}{L}q' \quad \text{for} \quad q' \leq q_1'. \tag{4.25}$$

These equations along with Equations (4.14) and (4.15) are implemented in a finite difference form on a digital computer to compare with experimental results in a later chapter.

Time Dependent Friction Model

For Newtonian fluids, Zielke [3] obtained an expression for the wall shear stress as a function of the past history of velocity gradients. Before Zielke, Szymanski [33] obtained an expression for the wall shear stress in terms of the past history of pressure gradients. It has been found that both expressions lead to the same result as far as predicting the pressure transients in a pipeline. However the approach based on velocity gradients is more convenient to implement than the one based on pressure gradients. For Bingham plastic fluids, as shown in the previous section, the wall shear stress unfortunately can not be represented as an explicit function of the average velocity. Hence, wall shear stress is evaluated based on the past history of pressure gradients instead of velocity gradients.

Atabek [16] developed an expression for the shear stress distribution across the cross section of a pipeline carrying a Bingham plastic fluid. He extended Szymanski's analysis technique to evaluate the shear stress for Bingham plastic fluid flow in a circular pipeline.

Atabek's approach is taken here to evaluate the wall shear stress for unsteady flow of pseudo-Bingham plastic fluid in a pipeline.

As before, the flow conditions at a cross section of the pipe is considered. All the assumptions made for deriving Equations (3.22) and (3.18) still hold. In addition, since pressure and flow at a cross section is considered, density variations are completely neglected along with the gravitational force term. Hence the continuity equation is identically equal to zero. The other equations become

z-Momentum:

$$\rho_0 \frac{\partial v_z}{\partial t} = - \frac{\partial p}{\partial z} - \frac{1}{r} \frac{\partial}{\partial r} (r \tau_{rz}) \tag{4.26}$$

$$\tau_{rz} = \tau_0 + \eta(- \frac{\partial v_z}{\partial r}) \quad \text{for} \quad \tau_{rz} \geq \tau_1 \tag{4.27}$$

and

$$\tau_{rz} = \mu_0 (- \frac{\partial v_z}{\partial r}) \quad \text{for} \quad \tau_{rz} \leq \tau_1. \tag{4.28}$$

The boundary condition is

$$v_z(R,t) = 0 \quad \text{for all } t.$$

Integrating Equations (4.27) and (4.28) and considering $\tau_{rz}(R,t)$

$$v_z(r,t) = \frac{1}{\eta} \int_r^R \tau_{rz} dr - \frac{\tau_0}{\eta} (R - r) \quad \text{for} \quad \tau_{rz}(R,t) \geq \tau_1 \tag{4.29}$$

and

$$v_z(r,t) = \frac{1}{\mu_0} \int_r^R \tau_{rz} dr \quad \text{for} \quad \tau_{rz}(R,t) \leq \tau_1. \tag{4.30}$$

Substituting Equations (4.29) and (4.30) for $v_z(r,t)$ in Equation (4.26) gives

$$\frac{\rho_0}{\eta} \int_r^R \frac{\partial \tau_{rz}}{\partial t} dr = - \frac{\partial p}{\partial z} - \frac{1}{r} \frac{\partial}{\partial r} (r \tau_{rz}) \quad \text{for} \quad \tau_{rz}(R,t) \geq \tau_1 \tag{4.31}$$

and

$$\frac{\rho_0}{\mu_0} \int_r^R \frac{\partial \tau_{rz}}{\partial t} dr = - \frac{\partial p}{\partial z} - \frac{1}{r} \frac{\partial}{\partial r} (r \tau_{rz}) \quad \text{for} \quad \tau_{rz}(R,t) \leq \tau_1. \tag{4.32}$$

Let $f(t) = - \frac{\partial p}{\partial z}$.

Differentiating Equations (4.31) and (4.32) with respect to r and rearranging gives:

$$\frac{\partial^2 \tau_{rz}}{\partial r^2} + \frac{1}{r} \frac{\partial \tau_{rz}}{\partial r} - \frac{\tau_{rz}}{r^2} - \frac{\rho_0}{\eta} \frac{\partial \tau_{rz}}{\partial t} = 0 \quad \text{for} \quad \tau_{rz}(R,t) \geq \tau_1 \tag{4.33}$$

$$\frac{\partial^2 \tau_{rz}}{\partial r^2} + \frac{1}{r} \frac{\partial \tau_{rz}}{\partial r} - \frac{\tau_{rz}}{r^2} - \frac{\rho_0}{\mu_0} \frac{\partial \tau_{rz}}{\partial t} = 0 \quad \text{for} \quad \tau_{rz}(R,t) \leq \tau_1. \tag{4.34}$$

The above two equations are alike except for the coefficient of the $\partial \tau_{rz}/\partial t$ term. If the pressure gradient is assumed to be a monotonically increasing function of time, then Equation (4.34) is valid at the wall until

$$\tau_{rz}\big|_{r=R} = \tau_1$$

and Equation (4.33) is valid for later times.

If $\tau_{rz}(r,0) = 0$ then the solution to Equation (4.34) is exactly the same as for Newtonian fluids [3]. This solution for the above initial condition is given by

$$\tau_{rz}(r,t) = \sum_{m=1}^{\infty} \frac{2}{R} \frac{\mu_0}{\rho_0} \frac{J_1(\frac{r}{R} z_m)}{J_1(z_m)} \int_0^t e^{-\frac{\mu_0}{\rho_0} \frac{z_m^2}{R^2} (t-\lambda)} f(\lambda)d\lambda. \qquad (4.35)$$

At the wall of the pipeline,

$$\tau_{rz}(R,t) = \tau_w(t) = \sum_{m=1}^{\infty} \frac{2}{R} \frac{\mu_0}{\rho_0} \int_0^t e^{-\frac{\mu_0}{\rho_0} \frac{z_m^2}{R^2} (t-\lambda)} f(\lambda)d\lambda. \qquad (4.36)$$

Let $t = t_1$ be the time at which $\tau_w = \tau_1$.

The differential equation that is valid at the wall is Equation (4.33) for $\tau_w \geq \tau_1$. The solution of this equation is same as the one for Equation (4.34) except that μ_0 is replaced by η. The initial condition is $\tau_{rz}(r,t_1)$. Then

$$\tau_w(t) = \sum_{m=1}^{\infty} \frac{2}{R} \frac{\eta}{\rho_0} \int_{t_1}^t e^{-\frac{\eta}{\rho_0} \frac{z_m^2}{R^2} (t-\lambda)} f(\lambda)d\lambda + \tau_1 \qquad (4.37)$$

$$\text{for } \tau_w \geq \tau_1 .$$

The above solution was obtained for an arbitrary but monotonically increasing input pressure gradient. The solution can be extended to a completely arbitrary input. The solution is represented in a slightly

different form for an efficient implementation on a digital computer. Let

$$\tau_w = \sum_{m=1}^{\infty} \tau_{wm} \tag{4.38}$$

where

$$\tau_{wm} = \int_0^t \frac{2\nu}{R} e^{-\frac{\nu}{R^2}(z_m)^2(t-\lambda)} f(\lambda)d\lambda. \tag{4.39}$$

If $\tau_w \leq \tau_1$, then $\nu = \frac{\rho_0}{\mu_0}$.

Otherwise $\nu = \frac{\rho_0}{\eta}$.

This is represented schematically in Figure 5. Equation (4.39) is the solution of the following first order differential equation with a zero initial condition.

$$\frac{d\tau_{wm}}{dt} + \frac{\nu z_m^2}{R^2} \tau_{wm} = \frac{2\nu}{R} f(t). \tag{4.40}$$

If Δt is the time step and input is constant for the duration of the step, then

$$\tau_{wm}(t + \Delta t) = \tau_{wm}(t)\, e^{-\frac{\nu z_m^2 \Delta t}{R^2}} +$$

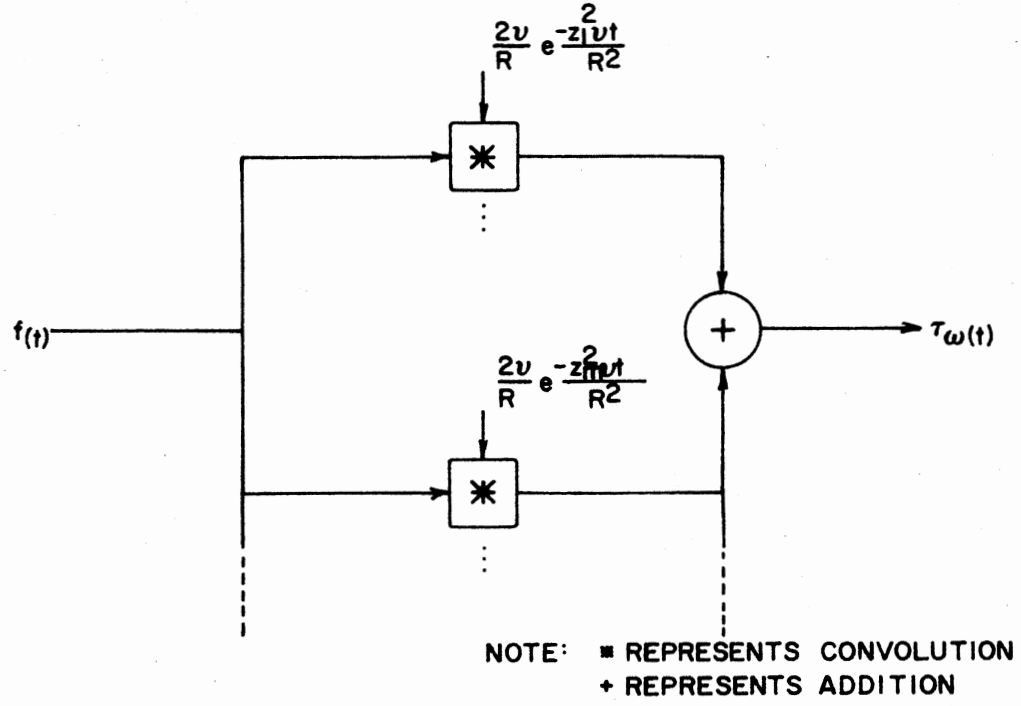

Figure 5. Block Diagram Representation of Convolution Integral for Wall Shear Stress Evaluation.

$$+ \int_t^{t+\Delta t} \frac{2\nu}{R} e^{-\frac{\nu z_m^2}{R^2}(t+\Delta t-\lambda)} Fu(\lambda)d\lambda \qquad (4.41)$$

which reduces to

$$\tau_{wm}(t + \Delta t) = \tau_{wm}(t)\, e^{-\frac{\nu z_m^2 \Delta t}{R^2}} + \frac{2}{z_m^2} FR\left(1 - e^{-\frac{\nu z_m^2 \Delta t}{R^2}}\right) \qquad (4.42)$$

and also

$$\tau_w(t + \Delta t) = \sum_{m=1}^{\infty} \tau_{wm}(t + \Delta t) \qquad (4.43)$$

The R.H.S. of the Equation (4.43) reduces to the following after rearranging

$$R.H.S. = \sum_{m=1}^{\infty} \left(\tau_{wm}(t) - \frac{2FR}{z_m^2}\right) e^{-\frac{\nu z_m^2 \Delta t}{R^2}} + \frac{FR}{2} \qquad (4.44)$$

$$\because \sum_{m=1}^{\infty} \frac{1}{z_m^2} = \frac{1}{4}.$$

To implement Equation (4.44) on a digital computer the following approximate expression is used to evaluate $\tau_w(t + \Delta t)$:

$$\tau_w(t + \Delta t) \simeq \sum_{m=1}^{N} \left(\tau_{wm}(t) - \frac{2f(t)R}{z_m^2}\right) e^{-\frac{\nu z_m^2 \Delta t}{R^2}} + \frac{f(t)}{2} R \qquad (4.45)$$

where N is a finite number and F=f(t).

The error involved in the evaluation of $\tau_w(t + \Delta t)$ using a finite number of terms is given in Appendix A. Due to slow convergence of the series, a fairly large number of terms is required for the evaluation of the wall shear stress $\tau_w(t + \Delta t)$. Normalizing Equation (4.45) with respect to p_f, and time with respect to the characteristic time t_c, gives

$$\tau_w'(t' + \Delta t') \simeq \sum_{m=1}^{N} \left(\tau_{wm}'(t') - \frac{2f'(t')}{z_m^2} e^{-\frac{\nu z_m^2 \Delta t}{R^2}}\right) + f'(t') \frac{R}{2L} \tag{4.46}$$

$$\text{where } \nu = \frac{\rho_0}{\mu_0} \quad \text{for} \quad \tau_w' \leq \tau_1' \tag{4.47}$$

$$\text{and } \nu = \frac{\rho_0}{\eta} \text{ otherwise.} \tag{4.48}$$

These equations are implemented on a digital computer in finite difference form to evaluate the time-dependent friction. The evaluation of the convolution integral could not be simplified any further (as Trikha [34] did for Newtonian fluids) due to the time varying nature of the parameter ν.

Constant Friction in Turbulent Flow

To predict the transient pressure response for the turbulent flow case, Equations (4.14) and (4.15) can still be used as long as the mean

velocity is considerably small compared to the velocity of sound and all other assumptions are the same as before. For the laminar flow case the wall shear stress can be calculated at any given flow rate or pressure gradient. However, in turbulent flow case an empirical relationship must be used to evaluate the wall shear stress. An algorithm is developed later in this section to evaluate wall shear stress based on steady-state friction factor vs Reynolds number charts obtained experimentally and correlated by Tomita [4]. Since the evaluation is based on the steady-state friction factor the method is similar in principle to the evaluation of wall shear stress based on steady-state friction in laminar flow. Using Tomita's approach to the evaluation of friction factor for turbulent flow case, the constant friction model developed earlier for the laminar flow case can be easily extended to the turbulent flow case.

The frictional losses in a pipeline due to the turbulent flow of a Newtonian fluid are indicated by the Fanning friction factor vs Reynolds number chart for different pipe wall roughness factors. Similar charts have been developed for certain classes of non-Newtonian fluids in the turbulent flow regime. For these classes, the effect of roughness of the pipe wall has not been considered as extensively as in the case of Newtonian fluids [14].

Development of Algorithm for Turbulent Flow Case

Tomita used the following definitions for friction factor and Reynolds number.

$$f = \frac{\pi^2 D^5 \Delta p}{32 \rho L q^2} (1 - c) \tag{4.49}$$

$$N_R = \frac{4\rho q}{\pi\eta D}(1 - c)\frac{(c^4 - 4c + 3)}{3} \tag{4.50}$$

Similarity considerations were used to deduce these expressions.

After rearranging Equation (4.21) using c, steady-state flow rate q through a pipeline is given by

$$q = \frac{\pi D^3}{32\eta}\frac{\tau_0}{c}\left(1 - \frac{4}{3}c + \frac{c^4}{3}\right) \tag{4.51}$$

Tomita used Equations (4.49) and (4.50) successfully to correlate the data for Bingham plastic fluids like slurries and muds on a single curve as shown in Figure 6. Tomita then applied Prandtl's mixing length theory to the turbulent flow of Bingham plastic fluids to obtain an empirical relationship between f and N_R. Due to the manner in which f and N_R have been defined, the relationship obtained is the same as in the case of Newtonian fluids. It is given by

$$\left(\frac{1}{f}\right)^{1/2} = 4 \ln (N_R \sqrt{f}) - 0.40 \tag{4.52}$$

Using Equations (4.49) and (4.52) the following algorithm is developed to find the wall shear stress τ_w for a given flow rate q. Pipe wall roughness is not considered in the following algorithm.

1. For given values of q,D, and η the constant c is to be determined using Equation (4.51). This equation is solved iteratively by back substitution.

2. The Reynolds number N_R is evaluated using Equation (4.50). If the value of N_R so determined is less than 2000, then the flow is assumed to be laminar and the wall shear stress is evaluated on that basis. If N_R is greater than 2000, then step 3 is executed.

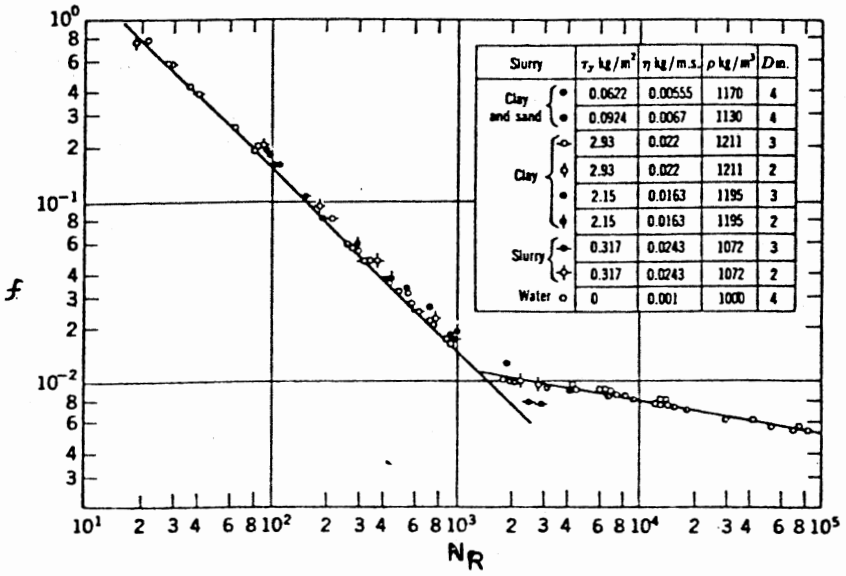

Figure 6. Experimental Correlations with Bingham Plastic Fluids in Turbulent Flow Regime [Tomita].

3. The friction factor f that corresponds to the Reynolds number N_R, is then obtained by solving Equation (4.52) numerically. Knowing f, Equation (4.49) is used to evaluate the wall shear stress τ_w as follows:

$$\tau_w = \frac{8\rho f(1 - c)q^2}{\pi^2 D^4} \tag{4.53}$$

Normalizing

$$\tau_w' = \frac{8\rho f(1 - c)q_f^2}{\pi^2 D^4} \frac{q'^2}{p_f} \tag{4.54}$$

Thus the algorithm makes it possible to evaluate equivalent wall shear stress for turbulent flow case. The constant friction model developed earlier for laminar flow case can easily be extended to turbulent flow case using this algorithm.

Implementation of the Method of Characteristics

Equations (4.14) and (4.15) can be implemented on a digital computer by rewriting them in a finite difference form. This form is valid along the characteristic grid lines as shown in Figure 7. It is assumed that the initial conditions and boundary conditions are specified. Considering the grid points I,J and K, Equations (4.14) and (4.15) become as follows:

$$\frac{P_J' - P_I'}{\frac{\Delta t'}{2}} + \frac{N_K}{\frac{\Delta t'}{2}} (Q_J' - Q_I') = -4\left(\frac{L}{D}\right) \tau_w' \tag{4.55}$$

when $\frac{\Delta z'}{\Delta t'} = +1$

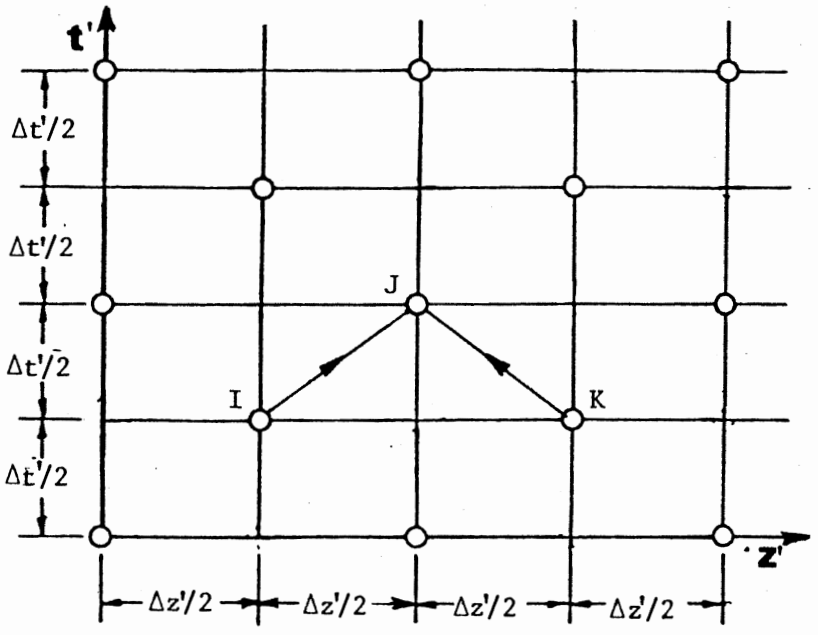

Figure 7. Fixed Grid for Method of Characteristics Solution.

and

$$-(P'_J - P'_K) + N_K(Q'_J - Q'_K) = -4\left(\frac{L}{D}\right) \tau_w' \tag{4.56}$$

when $\frac{\Delta z'}{\Delta t'} = -1$

These two equations can be solved for the unknowns P'_J and Q'_J knowing all other parameters. The wall shear stress is evaluated knowing Q'_I and Q'_K respectively if the constant friction model is used. For the evaluation of wall shear stress based on time-dependent friction, past history of pressure gradients corresponding to grid point J is used as indicated by Equation (4.46). A computer program listing for the implementation of the line models is shown in Appendix B.

CHAPTER V

EFFECT OF COLUMN SEPARATION

Column separation is a phenomena that occurs whenever the tension in a flowing liquid in a pipeline is large enough to break the liquid column into two columns. Under such tensions, the pressures at separation sections are very low and equal to the vapor pressure. Before column separation can occur, small cavities form as the pressure reduces. Earlier investigators assumed that these cavities are completely filled with vapor but later Schweitzer and Szebehely [27] showed that this is not necessarily true for all liquids. Their experimental investigations for several liquids including water showed that the cavities are occupied both by vapor and air. At any given pressure, liquid is saturated with a certain amount of dissolved air. When the pressure is reduced suddenly from the saturation pressure, air is released from the liquid. This explains the presence of air in the cavities. The percentage of dissolved air in water generally is very small whereas it may be much larger in other liquids such as Kerosene. Dissolved air appears to be the cause of formation of small cavity bubbles that appear whenever the pressure in water flowing in a pipeline falls below the saturation pressure. These bubbles grow in size as the pressure is reduced to vapor pressure, and the growth of these cavity bubbles is spontaneous near vapor pressure. Most of the cavity volume is then occupied by the water vapor. This appears to be the

reason why in earlier line models only vapor is considered to exist in the cavity and the effect of air in the cavity is neglected.

In previous chapters, equations were derived to predict the pressure transients in a pipeline carrying a pseudo-Bingham plastic fluid, in particular a coal slurry. The effect of column separation was not considered. Due to the presence of high pressure transients generated during water hammer, column separation will occur during the ensuing low pressure waves. Due to the presence of coal particles in water, it is assumed that water in a coal slurry is saturated with the air at ambient pressure. Whenever air pressure reaches a point near vapor pressure, a mixture of air and water vapor occupy the cavity volume. In this chapter, the Schweitzer and Szebehely' model for release of dissolved air from water is used to include the effect of column separation in the earlier derived pipeline dynamic model. Several elaborate techniques already exist in literature which treat the effect of dissolved air in water, but the one presented here is simple and computationally fast and appears to be quite satisfactory when predictions were compared with experimental results.

The amount of the air released in water at a given equilibrium pressure is given by the well-known Henry's law. It says that if no change in molecular structure occurs during the solution or evolution process, then the free volume of dissolved gas in the liquid is directly proportional to the absolute pressure.

$$V_e = s \frac{p_e}{p_0} V_\ell \tag{5.1}$$

Whenever the pressure of the air above the surface of the liquid

is reduced below the equilibrium pressure, and there is sufficient agitation, then the liquid is saturated at the new equilibrium pressure. Since the new equilibrium pressure is less than the previous equilibrium pressure, the mass of the air dissolved in the liquid is also less. If the volume of gas dissolved initially is V_1 at standard atmospheric conditions, and V_2 is the final volume of dissolved air, then the amount of evolved free air is given by

$$V = V_1 - V_2 \tag{5.2}$$

Sczweitzer and Szebehely associated a rate process with the evolution of air from the liquid whenever the gas pressure falls below the initial equilibrium pressure. By simple mathematical manipulations it can be shown that the amount of air evolved from t=0 to any time t, when the gas pressure above liquid surface is reduced from p_e to p_g, is

$$\Delta V = \frac{sn}{s+n} \left(\frac{p_e - p_g}{p_0}\right) V_\ell \left(1 - \exp\left(-0.693 \frac{t}{T_e}\right)\right) \tag{5.3}$$

So far only the evolution of gas from liquid is considered. When the gas pressure above the liquid surface goes above the initial equilibrium pressure then resolution of gas into the liquid takes place. This process is found to be considerably slower than the evolution process [27]. In the current work, resolution of gas into the liquid is not considered during the transients.

To obtain the volume of released air over one time step, Equation (5.3) is manipulated to yield the following

$$V_M = \frac{sn}{s+n}\left(\frac{p_e - p_g}{p_0}\right) V_\ell \tag{5.4}$$

$$V(t + \Delta t) = V(t) + (V_M - V(t))(1 - \exp(-\Delta t/T_c)) \tag{5.5}$$

where

$$T_c = \frac{T_e}{0.693} \tag{5.6}$$

As there is spontaneous growth in the cavity bubbles at or near vapor pressure, it is assumed that air release occurs only near the vapor pressure level. Also, the total pressure inside a cavity is the sum of the partial pressures due to water vapor and air. Once the air is released, it is assumed that it does not go back into solution with the water. With these assumptions, an algorithm can be implemented to consider the effect of column separation in the constant friction model using the method of characteristics solution technique. In Figure 7, grid points I, J, K are considered for illustration of the algorithm. The algorithm is applicable at all other grid points except the end grid points. The algorithm is as follows:

1. The pressure P_J and Q_J are evaluated using Equations (4.55) and (4.56). After making a correction for the gravitational force term, if the pressure P_J is less than the vapor pressure then the next step is executed. Otherwise, the same characteristic equations (4.55) and (4.56) are used to evalutate pressure and flow rate at grid point J.

2. Since P_J is less than the vapor pressure, P_J is set to the vapor pressure, and the cavity is allowed to form.

$$P'_J = P'_{VP} \tag{5.7}$$

Since the cavity exists at J, the flow rate is calculated assuming the volume as a boundary condition.

$$Q'_{J+} = \frac{1}{N_K} (P'_I - P'_J + Q'_I N_K - \frac{2L}{D} \tau'_{wI}) \tag{5.8}$$

$$Q'_{J-} = \frac{1}{N_K} (P'_J - P'_K + Q'_K N_K - \frac{2L}{D} \tau'_{wK}) \tag{5.9}$$

The increment in volume of the cavity can be found by the following integral:

$$\Delta V'_c = \int_{t-\Delta t}^{t} (Q'_{J-} - Q'_{J+}) dt. \tag{5.10}$$

This integral may be approximated to give

$$V'_c(t) = V'_c(t - \Delta t) + 0.5\Delta t(Q'_{J-}(t) - Q'_{J+}(t) + Q'_{J-}(t - \Delta t) - Q'_{J+}(t - \Delta t)). \tag{5.11}$$

When the cavity volume is positive and increasing, air release is considered. Otherwise there may not be any air release and the cavity is allowed to reduce in size.

For air release the following equations are implemented.

$$V_\ell = A\Delta z \tag{5.12}$$

$$\eta = \frac{V'_c}{V'_\ell} \quad \text{where} \quad V'_\ell = \frac{V_\ell}{V_f} \tag{5.13}$$

$$V'_M = \frac{sn}{s + n} (\frac{p_e}{p_{VP}} - 1) V'_\ell \tag{5.14}$$

$$V'_a(t) = V'_a(t - \Delta t) + (V'_M - V'_a(t - \Delta t))(1 - e^{-\frac{\Delta t}{T_c}}) \quad (5.15)$$

Equations (5.12) through (5.15) are assumed to be valid until the volume of air released is a certain fraction α of the total volume of cavity. It is assumed that the partial pressure due to air is negligible under those circumstances. Once the volume of air released exceeds α times the total volume of the cavity, air release is inhibited and a different set of equations is used.

3. When there is no more air release, an isothermal process is assumed and the volume of air follows the state equation

$$p'_{ca} V'_c = p'_{VP} V'_a \quad (5.16)$$

A more appropriate process would be the polytropic process, but since the equations considered using method of characteristics solution technique assume very small changes in temperature along the pipeline, the assumption of an isothermal process is justified. This assumption also has an incidental advantage of making the computations faster due to the simplicity.

The other equations that have to be solved along with Equation (5.16) are as follows:

$$P'_c = P'_{ca} + P'_{VP} \quad (5.17)$$

$$Q'_{J+} = \frac{1}{N_K} (P'_I - P'_c + Q'_I N_K - \frac{2L}{D} \tau'_{wI}) \quad (5.18)$$

$$Q'_{J-} = \frac{1}{N_K} (P'_c - P'_K + Q'_K N_K - \frac{2L}{D} \tau'_{wK}) \quad (5.19)$$

In addition, Equation (5.11) is used to update the volume of the cavity. While using these equations if the pressure in the cavity becomes less than $(1 + \alpha)\, p_{VP}$, then step 2 of the algorithm is implemented.

From the algorithm above, it can be observed that air is released very sparingly since no more air release occurs once the partial

pressure of the air is greater than α times the vapor pressure. For this study with coal slurry, an average α of 0.08 was chosen.

In actual implementation on the digital computer, the solution became unstable when the ratio equals to 1. This instability is attributed to the fact that the approximate integral used for integration of the flow rate difference to obtain the volume of the cavity is not accurate at the given time step, especially when large changes in volume occur. This has also been observed by others when the amount of air release is small [2,28]. One or both of the approaches below are to be taken in such a case.

1. The time step is reduced further and the simulation is carried out again. However, as the time step is reduced by some factor, the number of grids is increased by the same factor and greater number of calculations needs to be performed.

2. The time step is reduced but the number of grids is not changed. This means that $\Delta z'/\Delta t'$ can be greater than one. It suggests interpolation between grids to obtain the values of the pressure and flow rate variables. This procedure is shown diagramatically in Figure 8. By using interpolation technique, the grid size is made independent of time step Δt, as long as the ratio $\Delta z'/\Delta t' > 1$[1]. However this interpolation technique introduces numerical damping in the solution. To minimize the numerical damping the ratio $\Delta z'/\Delta t'$ should be very close to unity. So the ratio that is greater than unity, closer to unity, and that makes the solution to converge is chosen.

---

[1]Courant's criterion.

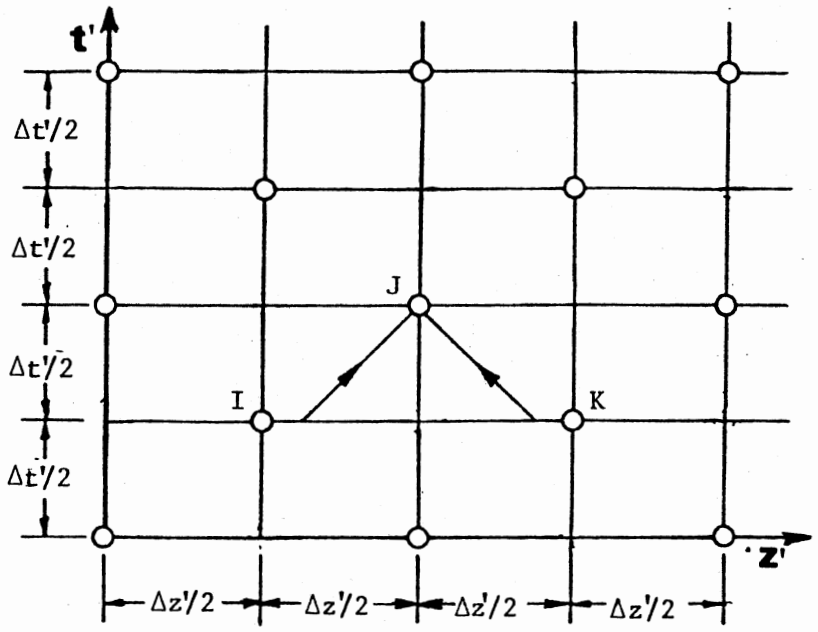

Figure 8. Illustration of Interpolation Between Grids in Method of Characteristics Solution Technique.

CHAPTER VI

VALIDATION OF THE MODELS

An experimental study was conducted to validate the use of the pseudo-Bingham plastic model for predicting pressure transients in a coal slurry pipeline. In particular, the objective was to validate the constant friction models developed for the laminar and turbulent flow regimes with and without column separation, and the time-dependent friction model for the laminar flow regime. A schematic of the experimental setup is given in Figure 9. The following factors were considered in the selection of the test line length and diameter.

1. The L/D ratio should be much greater than unity. One dimensional analysis is justified only when this condition is satisfied.

2. The valve closure time should be less than the wave propagation time 2L/a. This ensures that the pressure peak amplitude obtained at the upstream end of the valve is the maximum for a given initial steady flow. This ensures high frequency content in the response and also makes it possible to assume quick closure as the boundary condition in the line model. The quick closure assumption eliminates the need to consider time of closure and valve characteristics in the model.

Experimental Setup

A schematic of the experimental test section is shown in Figure 9. The setup consists of a 1/2 in. I.D. galvanized steel tube having a length of 496.6 inches. The pressure source for the line is a pressure

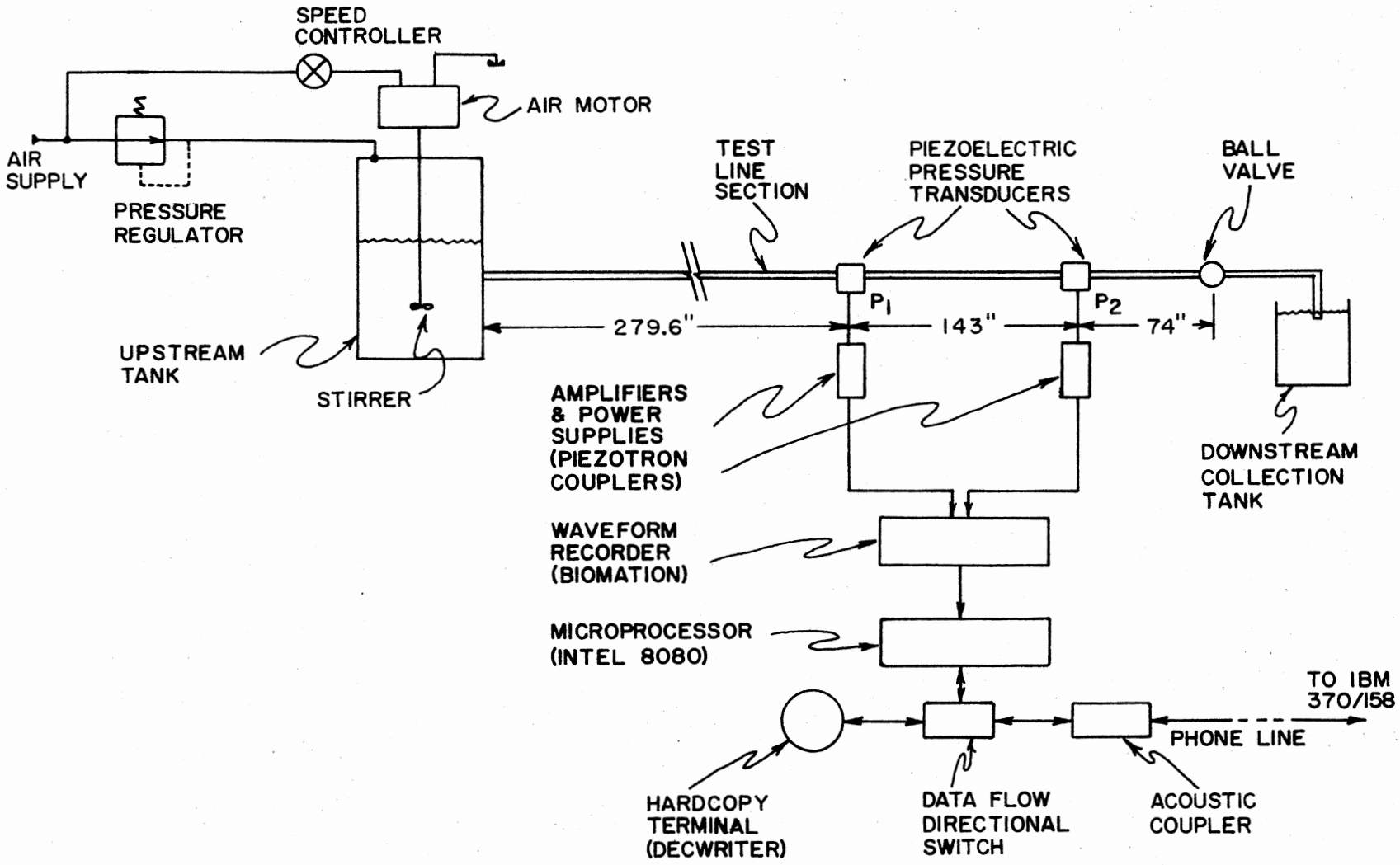

Figure 9. Schematic of the Experimental Setup

tank having an inside diameter of 14 in. and a height of 28 in.. The lid on the tank supports a stirrer rod that can be turned by an air motor mounted on the top of the lid. The speed of the motor can be varied. Stirring action is provided by a two blade stirrer that is attached to the other end of the rod. Fluid is introduced into the tank from the top. The tank is pressurized with air. By maintaining constant air pressure using a regulator, steady flow can be established through the test line at low flow rates. The downstream end of the line is connected to a receiving tank using a flexible hose.

Two piezoelectric transducers are mounted on the test line to obtain the pressure response at two different locations. These transducers are flushmounted on the line. A cross sectional view of the transducer mount is shown in Figure 10. The outputs from the transducers are connected to a waveform recorder. The digital output of the recorder is sent to a microprocessor (INTEL 8080) which in turn transmits data by phone line to a digital computer (IBM 370/158). Data processing is then done on the digital computer.

Experimental Procedure

The pressure transducers were calibrated using the step pressure change obtained by pressurizing the line and suddenly opening the downstream valve. A calibration error of $\pm$11 percent was detected using this method of calibration.

Coal which is ground to a nominal size of 100 microns was used to prepare the coal slurry. The actual size distribution of the particles is shown in Table I. Pulverized coal was then mixed with water approximately in 50:50 proportion (by weight). The exact proportion is

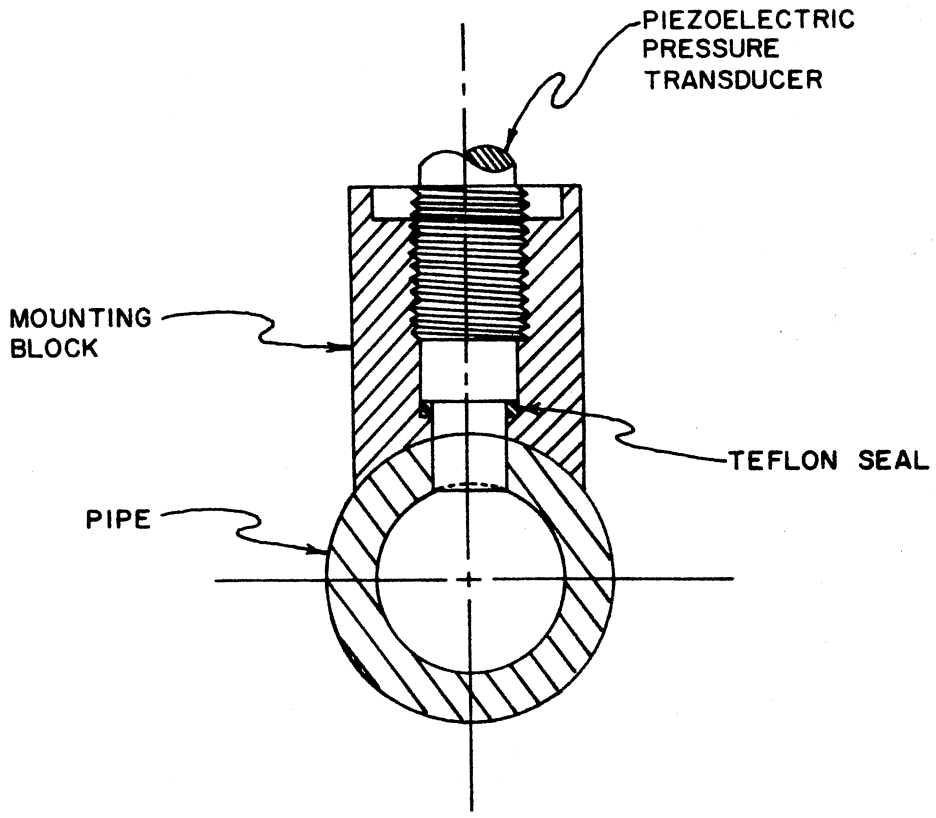

Figure 10. Cross Sectional View of the Transducer Mount

TABLE I

SIEVE ANALYSIS OF COAL USED IN EXPERIMENTS

Retained on	Passed thru		Percent
#50	----		1.13
#60	#50		2.57
#100	#60		24.90
#200	#100		32.30
----	#200		39.10
		TOTAL	100.00

reported along with the experimental response. The rheological characteristic of the coal slurry was obtained using a Fann viscometer (rotary viscometer). The results are shown in Figure 11. The choice of the particle size and concentration was dictated by the earlier reports of the rheological characteristics of coal slurries prepared with different particle sizes and concentrations of coal in water by Faddick [1]. Existing commercial long distant coal slurry pipelines use approximately the same concentration as Faddick with a slightly higher percentage of particles of coal above the 100 microns size. From the rheogram shown in Figure 11, it can be seen that the test coal slurry behaved approximately like a pseudo-Bingham plastic fluid.

After the rheological characteristics were measured the slurry was then poured into the tank to conduct the experiments. Before taking the measurements, the slurry was run through the pipeline to purge the line of air bubbles trapped in the line. A measurement of the velocity of sound in the slurry indicated the extent of air trapped in the pipeline. The slurry collected at the downstream was then recycled prior to the beginning of the basic tests.

Experimental data was obtained for different operating conditions.

Sudden Valve Closure With no Column Separation

Initially, steady flow was established. The flow rate was chosen such that the pressure in the line did not reach the vapor pressure at any instant of time following sudden closure of the ball valve at the downstream end of the test line. Experiments were performed with flow rates between 0.2 to 0.8 cubic inches per second which was always greater than the settling velocity. After establishing the required

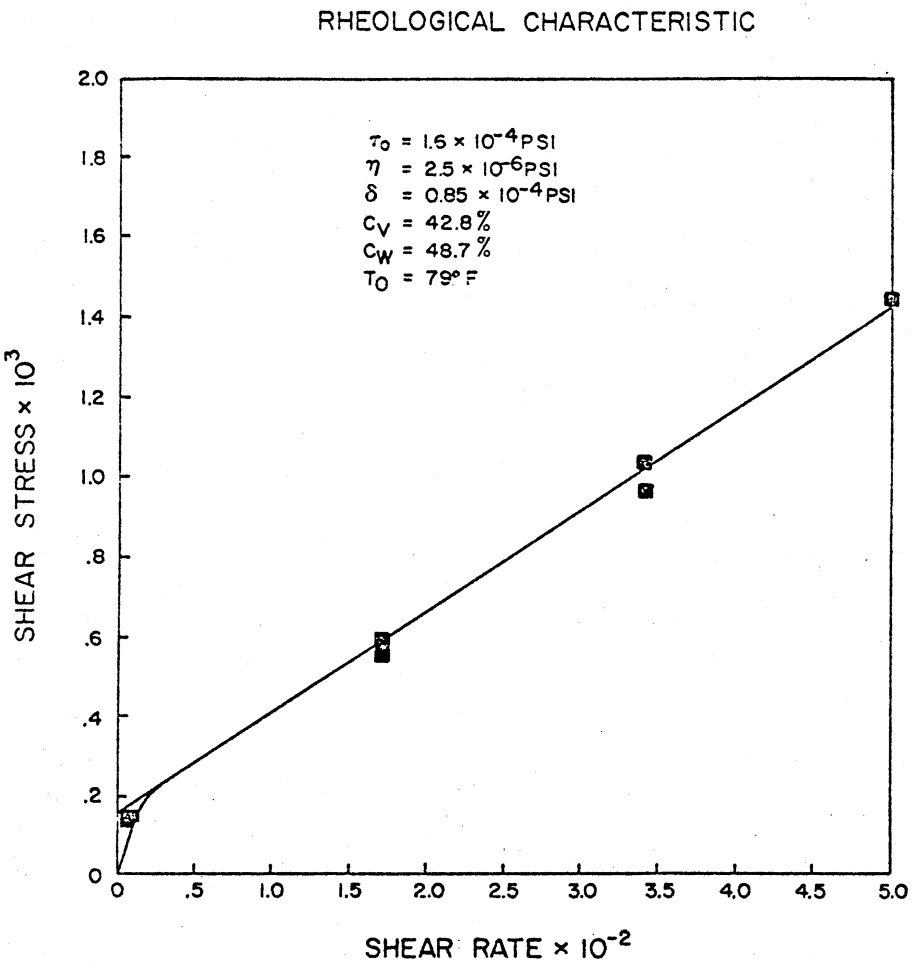

Figure 11. Rheological Characteristic of a Coal Slurry.

steady flow, the valve was suddenly closed and at the same time the waveform recorder was triggered to record the output voltage response of the two pressure transducers. Using the microprocessor the data was then transmitted from the waveform recorder to the digital computer over phone lines. Typical output responses are shown in Figure 12.

An evaluation of the first peak amplitude based on initial steady-state flow rate showed that the valve closure was indeed a sudden closure i.e. valve closure time is less than 2L/a seconds. The apparent large difference between the first peak amplitudes at the transducers 1 and 2 is attributed to the calibration errors in transducers 1 and 2. The vibrations caused by valve closure can be seen to be negligible.

Sudden Valve Closure With Column Separation

As in the experiment described above, steady flow was established initially. Cavitation followed sudden valve closure whenever the flow rate was higher than about 1.5 cubic inches per second. Flow rates between 1.5 to 2.5 cubic inches per second were chosen so that the flow remained laminar and the maximum pressure peak was within the measurable range of the pressure transducers. Pressure responses of the transducers were recorded immediately after quick closure of the ball valve. Typical responses are shown in Figure 13. Again the initial peak amplitude evaluation based on the initial steady-state flow rate confirmed that the valve was closed suddenly. The negative pressure peak reached the vapor pressure level of water indicating cavitation in the line. It can also be observed that the duration of the negative pressure peaks is longer than the duration of the positive peaks indicating possible column separation.

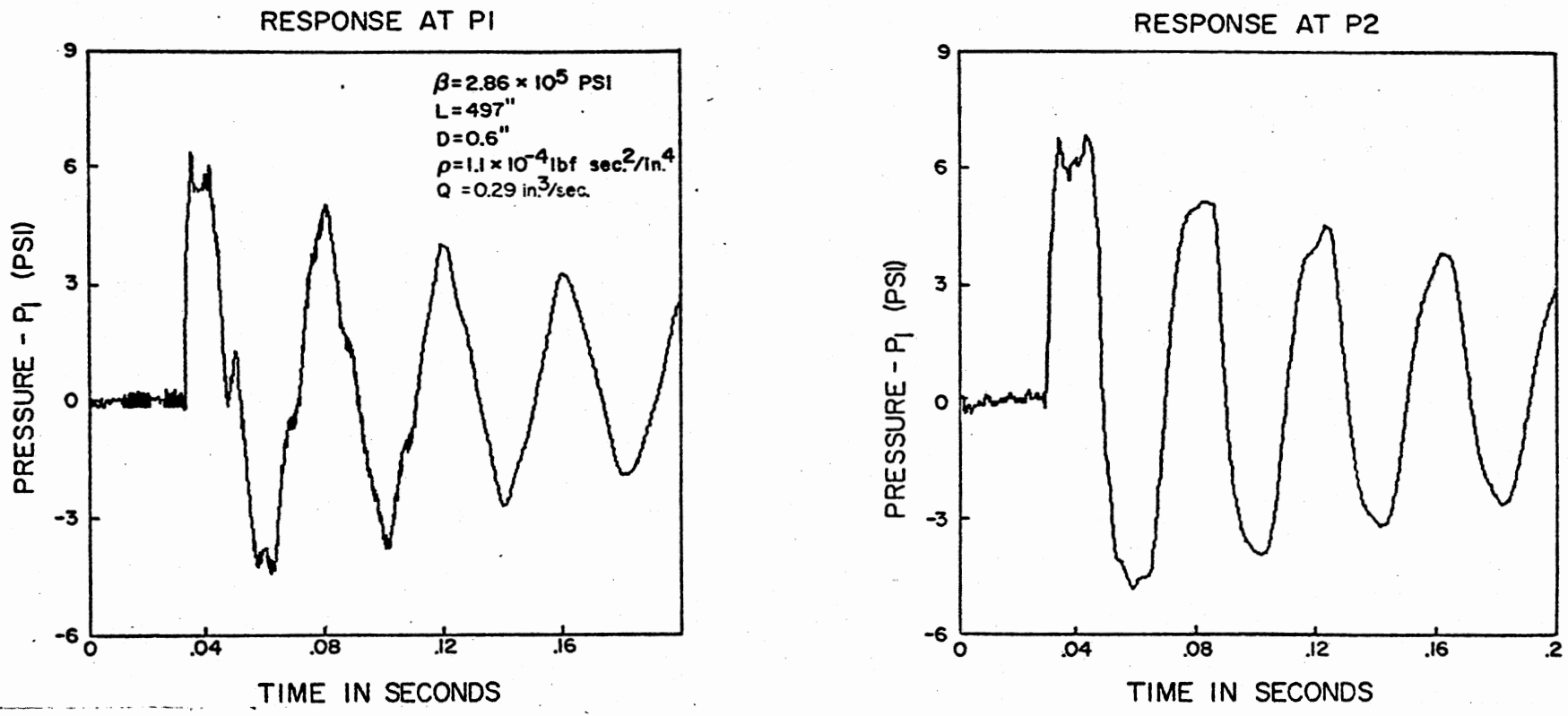

Figure 12. Experimental Response for Quick Valve Closure (No Column Separation)

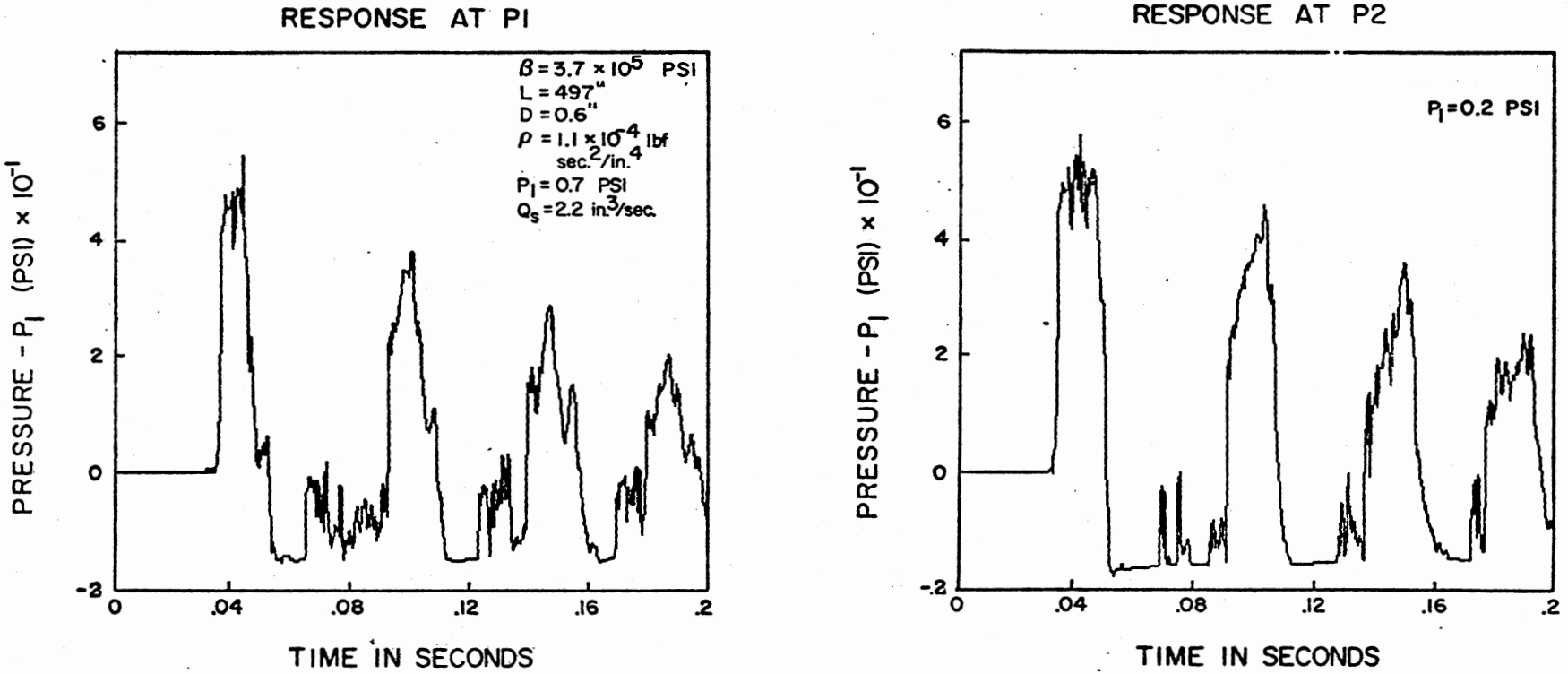

Figure 13. Experimental Response for Quick Valve Closure (Column Separation)

Sudden Valve Opening

This particular boundary condition for the downstream end of the line was selected to validate the constant friction model in turbulent flow regime. Sudden valve closure cannot be used because of the occurrence of cavitation and the accompanying column separation at high flow rates. Initially steady flow was established at a supply pressure of about 50 psi. Then the valve was closed slowly until there was no flow in the pipeline. The supply pressure was then raised to a higher value and the valve was opened suddenly. The pressure transients were recorded and processed as before. Typical responses appear in Figure 14.

The velocity of sound was obtained from the experimental response itself by measuring the round trip travel time of the wavefront from a transducer. Due to the presence of a varying number of small air bubbles, the velocity of sound differed in a small degree from one experimental response to another. The velocity of sound for a given experimental response is higher at the start of the transient and reduces slightly as time elapses. This slight decrease in the velocity of sound is a function of the amount of air released from the slurry. An average velocity of sound can be established for a given experimental response.

Independent measurements were made on other parameters like density, length of the line, diameter of the line, etc. With the measured parameter values, the line models developed earlier were used to predict the theoretical pressure responses. The predicted pressure responses are compared with the experimental pressure responses in the following subsections.

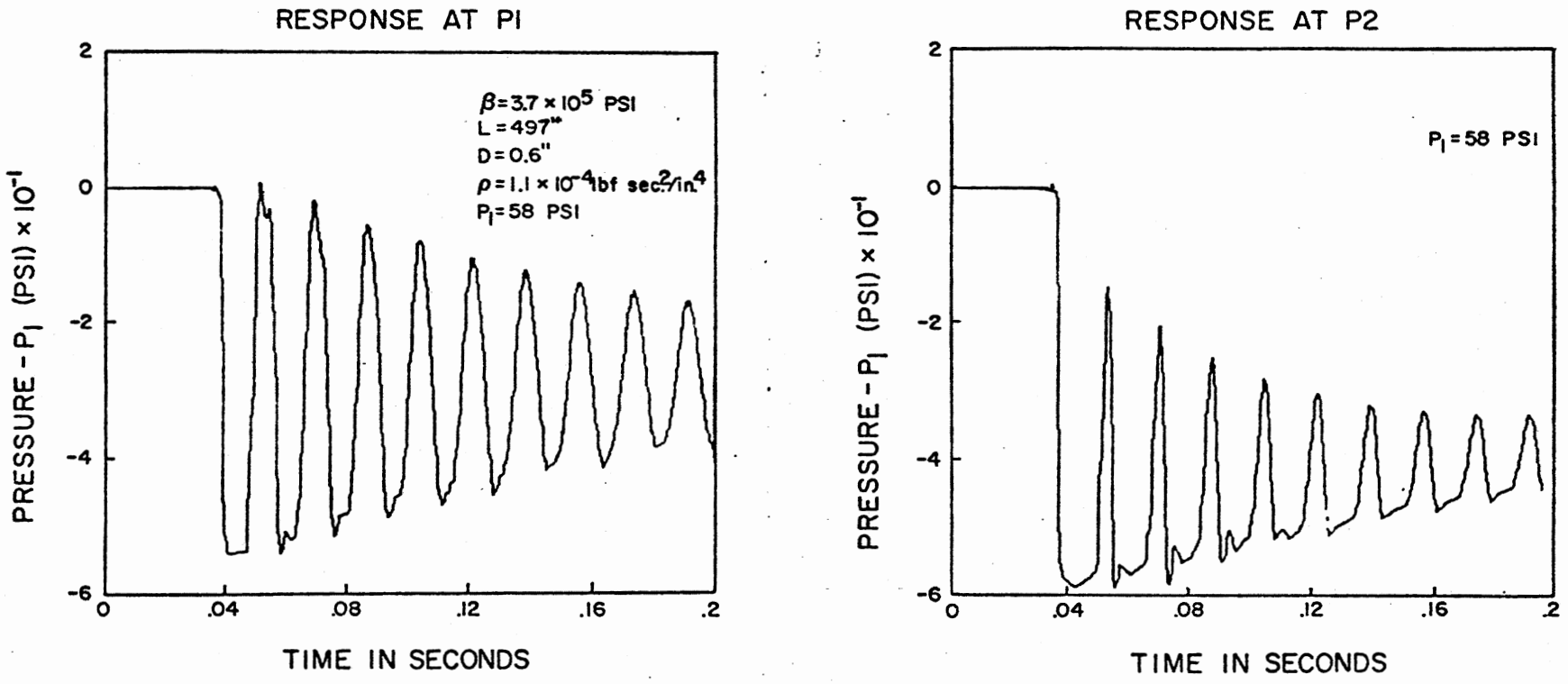

Figure 14. Experimental Response of Coal Slurry for Sudden Valve Opening

Comparison with Dynamic Models

The dynamic models were used to simulate the experimental operating conditions.

Case 1 - Sudden Valve Closure with no Column Separation

The pressure responses at transducers 1 and 2 were predicted using the simple constant friction model discussed in Chapter IV for this operating condition. A predicted response and an experimental response are superimposed in Figure 15.

The boundary conditions for the model were assumed to be a constant pressure source at the upstream end of the line and a quick valve closure at the downstream end. The time step and the number of grids used in the method of characteristics solution technique are given in the same Figure 15.

The model predicts the maximum values of both positive and negative pressure peaks fairly accurately using the measured values for yield stress τ_0 and coefficient of plasticity η, each of which has a measurement error of at least ±10 percent. Since constant friction is assumed, the attenuation of all the frequency components of the wave front is constant. However, from the experimental response it is evident that this assumption is not valid. This error is the main drawback of the constant friction model. However, computationally the constant friction model takes less time on a digital computer. In applications such as in preliminary design of slurry pipelines where only approximate values of the peak amplitudes are needed, the

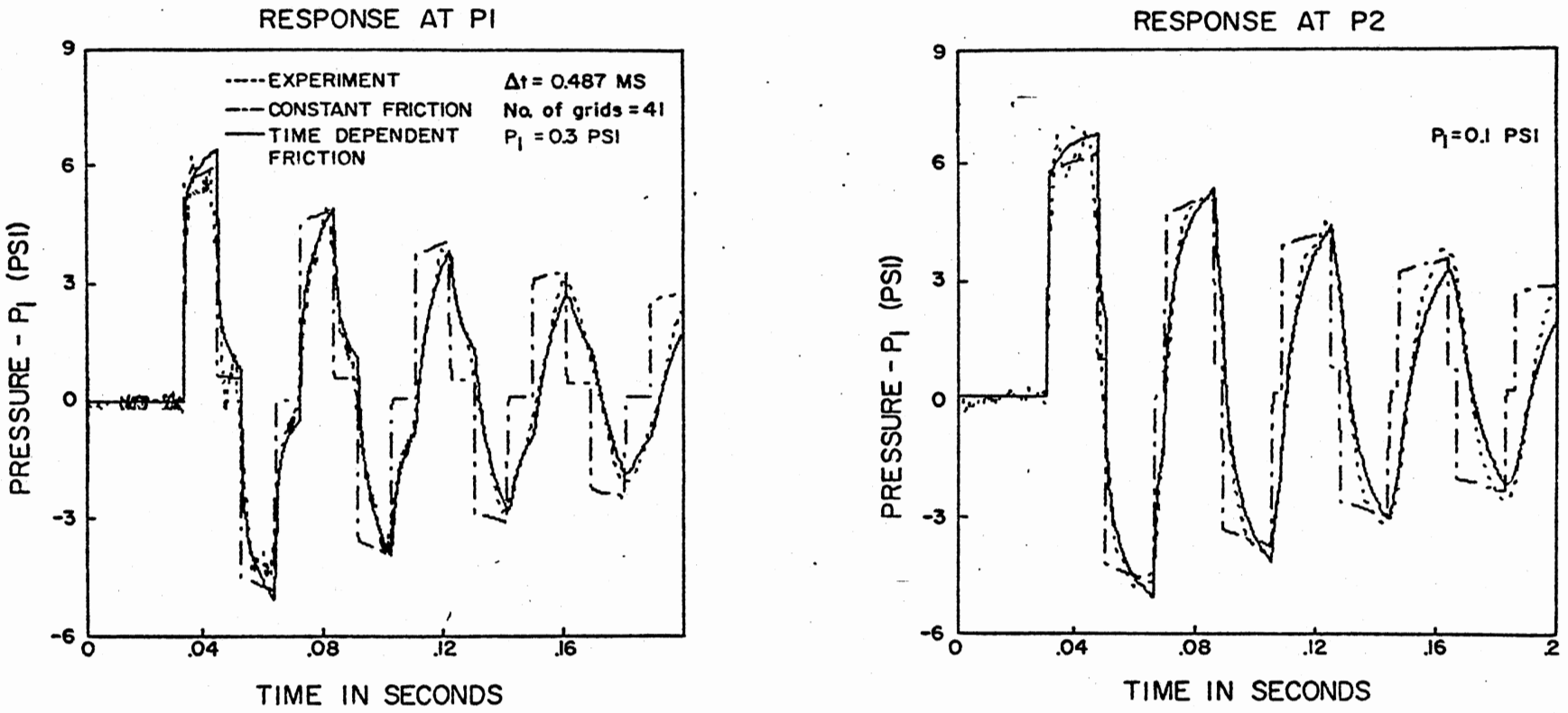

Figure 15. Comparison Between the Predicted and Experimental Responses for Quick Closure with no Column Separation

constant friction model can be useful and efficient. A comparison of the predictions using the constant friction model based on Newtonian fluid assumption with the same experimental response is shown in Figure 16. The apparent viscosity μ_a was calculated from the measured rheological characteristic using the following equation.

$$\mu_a = \eta + \frac{\pi \tau_0 D^3}{24Q} \tag{6.1}$$

Initial steady flow rate was used in calculating μ_a. The discrepancy in peak amplitude prediction can be observed.

A comparison of the response obtained using the time-dependent friction model with the experimental data shows that dispersion of the wave front is predicted reasonably well. The time-dependent friction model for a pseudo-Bingham plastic fluid considers the past history of pressure gradients for the wall shear stress evaluation. In contrast, the past history of velocity gradients is used in the time-dependent friction model for Newtonian fluids [3].

The predicted response matches very closely with the experimental response in spite of the approximations made in developing the model. The model has to be validated with different fluids or coal slurries that have higher yield stress and a different coefficient of plasticity. The time-dependent friction model can be used in applications where the attenuation characteristic of the pressure waves needs to be known very accurately e.g. like in a critical pipeline design.

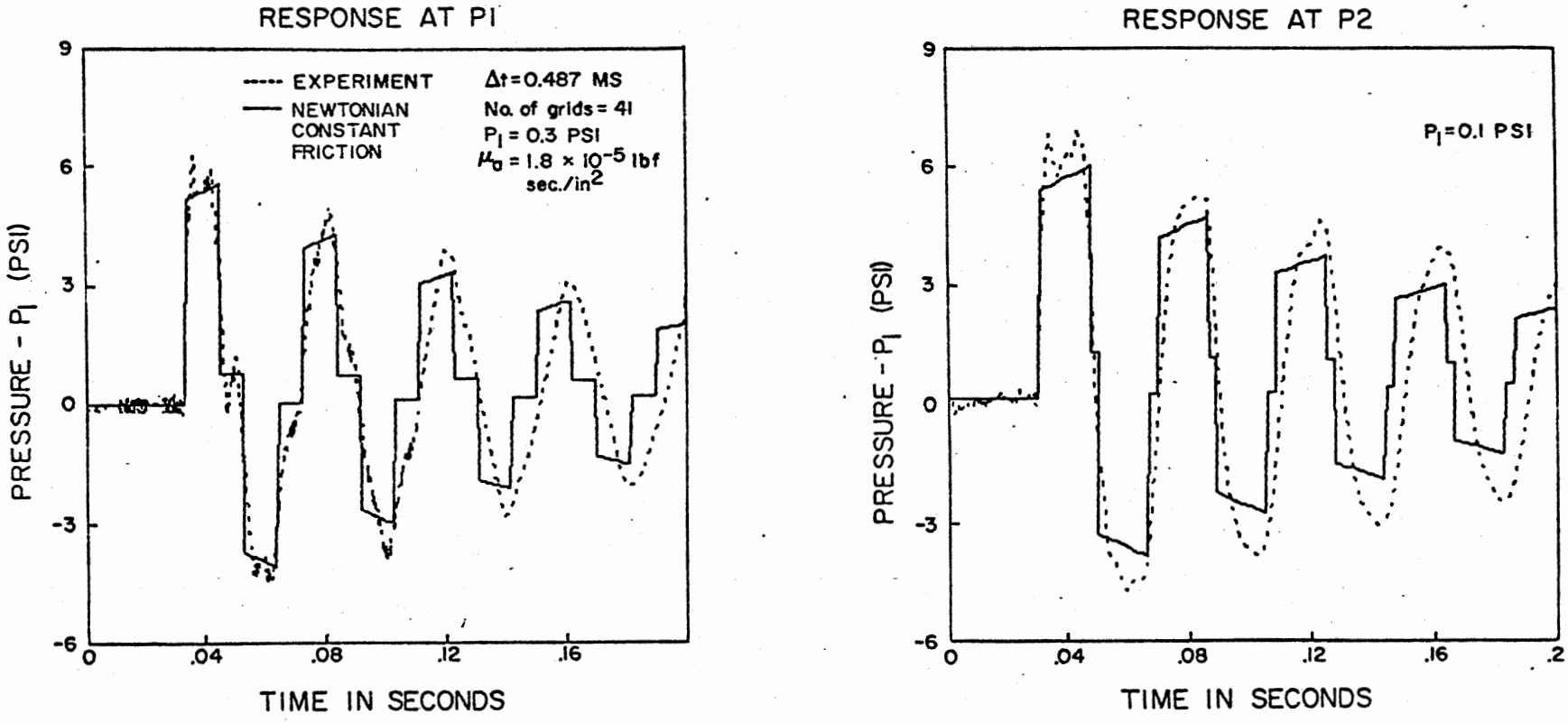

Figure 16. Comparison of the Predicted Response Based on Newtonian Fluid Assumption with the Experimental Response for Quick Closure with no Column Separation

Case 2 - Sudden Valve Closure with Column Separation

In this case, the constant friction model with the cavitation model included, was used to predict the transient pressure response when there is column separation in the pipeline. Predicted and experimental responses are shown in Figure 17.

All the parameters were measured separately, except the two parameters that are needed for simulating the cavity growth model. These two parameters viz. solubility constant s and air release time constant T_c, are obtained from the published data by Schweitzer and Szebehely [27] for water. The initial flow rate is high enough to cause cavitation at the upstream end of the valve after 2L/a seconds upon valve closure.

A comparison of predicted and experimental responses shows good agreement between model and experiment. Convergence of the numerical solution was obtained for $\Delta t'/\Delta z'$ equal to 0.75. Any reduction in the ratio $\Delta t'/\Delta z'$ results in more damped response. However the times of occurrences of the peaks are predicted to the same accuracy, even if the ratio $\Delta t'/\Delta z'$ is reduced to a smaller value. Experimental responses matched with theoretical responses for different initial flow rates once the ratio $\Delta t'/\Delta z'$ was properly chosen for the numerical solution to converge. Almost all the models presented in the literature related to cavity growth in liquids with low solubility coefficients, are poor in predicting the pressure peaks that occur after the first and second peak. The cavity growth model developed here for liquids with low solubility coefficients appears to describe the cavity growth process

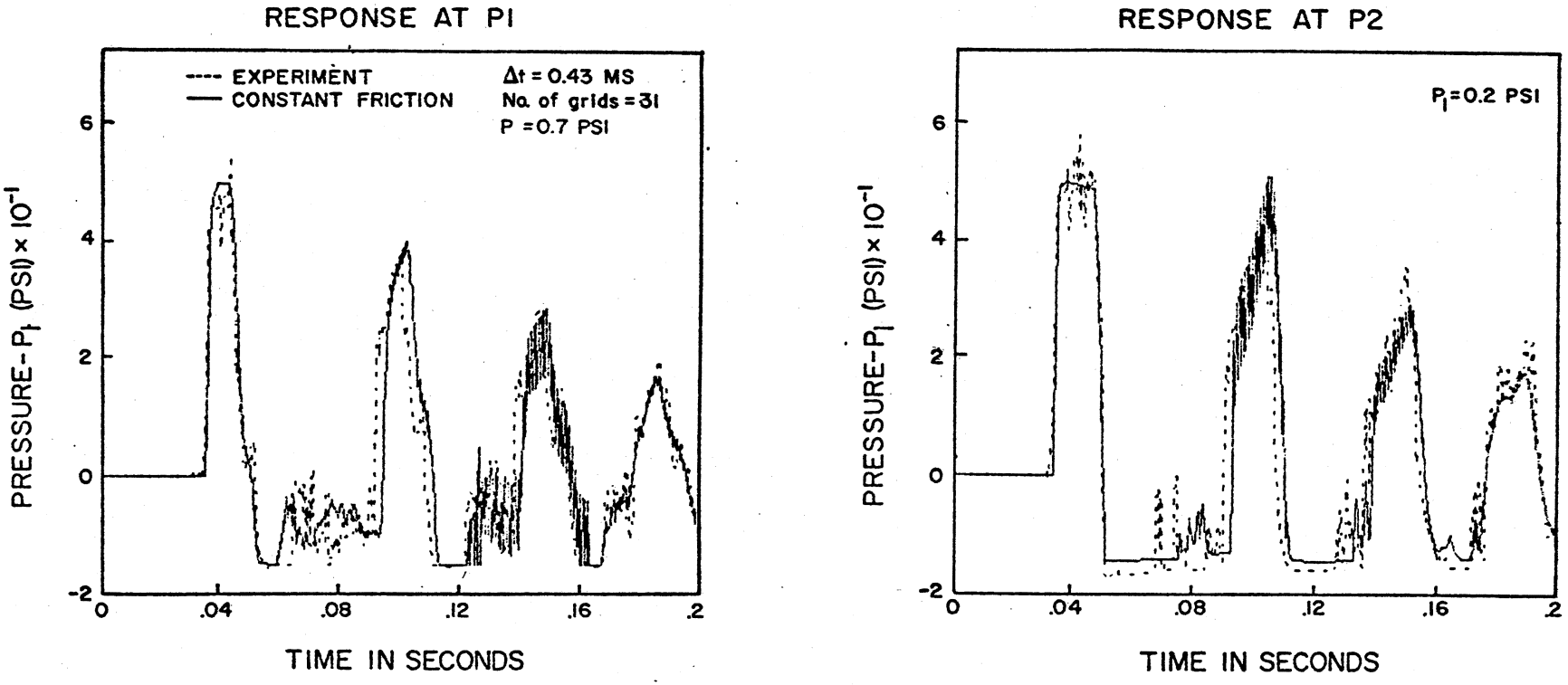

Figure 17. Comparison Between the Predicted and Experimental Response for Quick Closure with Column Separation

more realistically. It can be seen that not only the first two peaks but also the latter peaks matched both in amplitude and time of occurrence. The liquid, in the present case a coal slurry, had very few air bubbles at the start of the test. This result is evident from the initial high velocity of sound. Also the velocity of sound is assumed to be constant in the model. Since the amount of released air is small, this assumption is justified as evidenced by the experimental results.

Case 3 - Sudden Valve Opening

The simple constant friction model was extended to turbulent flow regime in Chapter IV. An experimental response for turbulent flow regime was obtained as outlined in the experimental procedure under the subsection for sudden valve opening. The transient responses thus obtained are compared with the theoretical predictions in Figure 18. A sudden jump in attenuation can be observed in the theoretical response. This is due to the change in the evaluation procedure for friction, when the Reynolds number for the slurry exceeds 2000. It is assumed in the model that the laminar to turbulent transition occurs at a Reynolds number of 2000. No such jump in attenuation occurs in the experimental response. It is possible that the flow did not become turbulent at a Reynolds number of 2000 as assumed by the model. Also, the flow may have become turbulent gradually, but not as suddenly as depicted by the predicted response. It is hard to determine when the flow has become turbulent for a transient flow. Because of these difficulties, no model has been developed that can predict the transients as accurately as the models that have been developed for laminar flow regime.

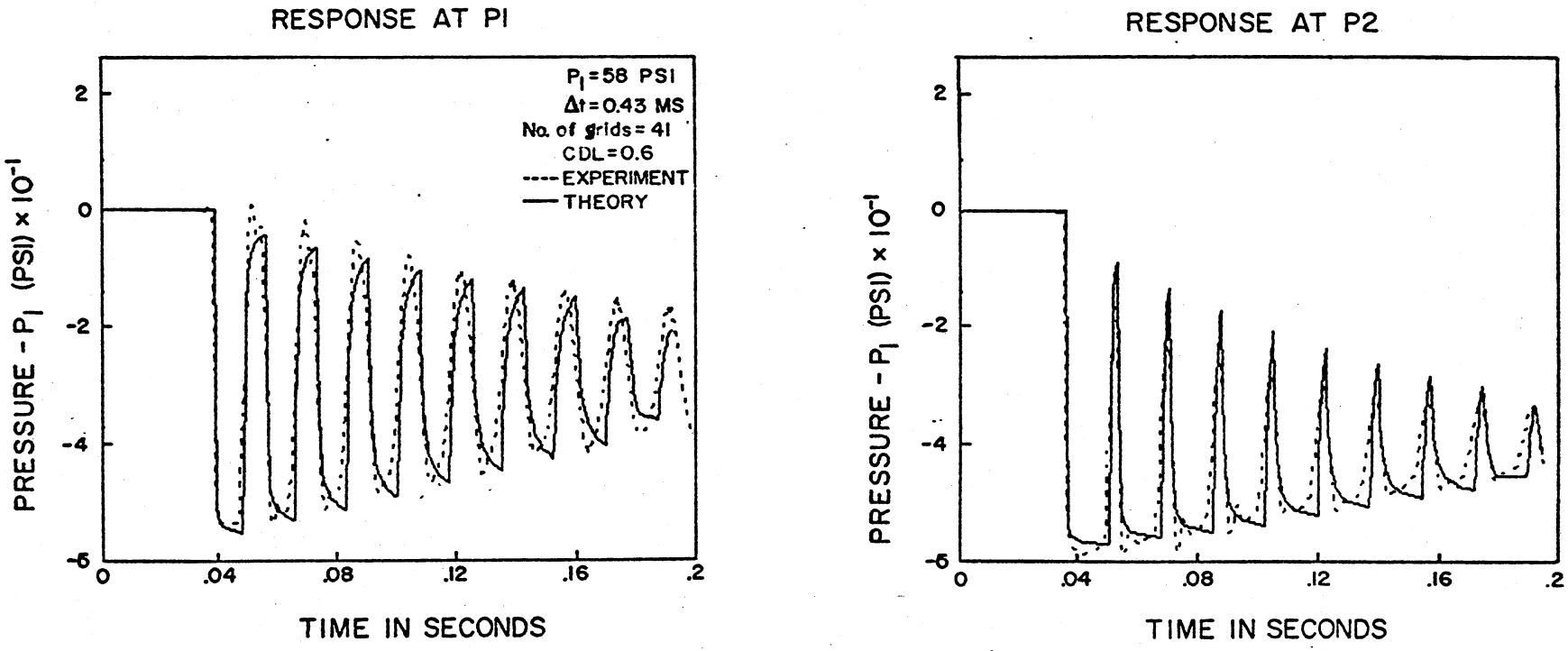

Figure 18. Comparison Between the Predicted and Experimental Response for Sudden Valve Opening

An objective of the current dissertation was to extend the steady-state friction model developed for the laminar flow regime to the turbulent flow regime to take into account the increased attenuation at higher flow rates. A similar extension was done for Newtonian fluid pipeline models. The model developed in Chapter IV is intended to be only an aid in predicting the approximate pressure peak amplitudes during transient conditions when the flow becomes turbulent. Comparing the experimental and predicted results for the condition when the steady flow is at least twice as high as the flow rate corresponding to the Reynolds number of 2000, it can be concluded that the constant friction model indeed can serve as a design tool in approximately predicting the pressure peaks that occur during transients.

CHAPTER VII

CONCLUSIONS AND RECOMMENDATIONS

A simple constant friction model and a time dependent friction model have been developed for predicting the transient pressure and flow responses in a pipeline carrying a pseudo-Bingham plastic fluid such as coal slurry, mud etc. These models have been validated with experimental data obtained from a prototype pipeline using coal slurry. Validation of these models suggests that the assumptions made in developing the models are justified, especially the manner in which the rheological characteristic of the pseudo-Bingham plastic fluid is implemented in the constant friction and the time dependent friction models. Although it can be argued that treating a pseudo-Bingham plastic fluid as a Newtonian fluid whose viscosity is equal to the apparent viscosity may give rise to results that are adequate for some purposes, such a treatment may not be justified for a critical pipeline design application. Also, since the apparent viscosity is a function of the velocity at the operating conditions, the Bingham plastic fluid rheological model must be used to calculate the velocity. The implementation of the non-Newtonian fluid constant friction model on a digital computer is as easy as the implementation of the constant friction model based on Newtonian fluid assumption.

A comparison of model predictions with experimental data shows that the time dependent friction model is much better in predicting the

transient pressure response than the constant friction model. However the computation time for the former is much higher than that required for simulating the constant friction model. Though these models have been validated with a coal slurry having a known composition, their validity for different compositions of coal slurry and for different pseudo-Bingham plastic fluids can only be confirmed by conducting more experiments.

A cavitation model that allows release of dissolved air from the water has been included in the constant friction model. This cavitation model is only for liquids that have a low solubility coefficient. The cavitation model is conservative in that air is released only when the pressure at any point reaches the vapor pressure. Also, the cavities are assumed to be formed only at the grid nodes. The velocity of sound is held constant in the model. With these assumptions, the theoretical predictions using the cavity growth model correlated surprisingly well with the experimental data. This agreement suggests that the macroscopic modelling of the cavitation mechanism is appropriate for the coal slurry under consideration. No general conclusion about the validity of the model can be made unless more experiments are performed with different fluids having low solubility coefficients. Since the objective was to develop a computationally fast, yet reasonably accurate model to predict the column separation in a coal slurry pipeline, no attempt is made to validate the model with different fluids having different solubility coefficients.

The constant friction model has been extended to the turbulent flow regime using Tomita's experimental correlations for Bingham plastic fluids. A comparison of predictions with experimental results

confirmed that a model that considers the steady-state turbulent friction is better than the one that considers only steady-state laminar friction.

Overall, the models are valid within the experimental error bounds and within the constraints imposed in the model development. The experimental results do provide some confidence in the line models developed.

The following are a few recommendations to further the present work.

1. Study the effect of concentration and particle size on the parameters such as yield stress, and coefficient of viscosity.

2. Study the effect of the solubility coefficient and undissolved air bubbles on the experimental response to establish the range of validity of the cavity growth model developed.

3. Develop a design procedure for synthesizing coal slurry and for specifying the pipeline requirements making use of the dynamic line models in addition to steady-state models. This design should be optimum in terms of cost, efficiency and resource management.

SELECTED BIBLIOGRAPHY

(1) Faddick, R.R. "Flow Properties of Coal-Water Slurries." Third International Conference on the Hydraulic Transport of Solids in Pipes, Hydraulic Transport of Solids in Pipes, Hydraulic Transport 3, 15th - 17th May 1974, pp. H1.1-H1.6.

(2) Wylie, E.B., Streeter, V.L. Fluid Transients. New York: McGraw Hill, 1978.

(3) Zielke, W. "Frequency Dependent Friction in Transient Pipe Flow." Journal of Basic Engineering, ASME Trans., Series D, Vol. 90 (March, 1968), pp. 202-208.

(4) Tomita, V. "Study on Non-Newtonian Flow in Pipe Lines." Bull. of JSME., Vol. 2 (1959), pp. 10-16.

(5) Sacks, M.E., Romney, M.T., and Jones, J.F. "Some Pumping Characteristics of Coal Char Slurries." Ind. Eng. Chem. Process Res. Develop., Vol. 9 (January, 1970), pp. 148-153.

(6) Buckingham, E. Proc. ASTM., Vol. 21 (1921), pp. 1154-1161.

(7) Reiner, M. Deformation and Flow. Lewis, London: Interscience Publ., 1949.

(8) Reiner, M. "Phenomelogical Macrorheology." Chapter 2 in Rheology, Eirich F.R. (Ed.), New York: Academic Press, Vol. 1 (1956), p. 45.

(9) Bain, A.G., and Bonnington, S.T. The Hydraulic Transport of Solids by Pipeline. New York: Pergamon Press, 1970.

(10) Caldwell, D.H., and Babbit, H.E. "Flow of Muds, Sludges, and Suspensions in Circular Pipe." Ind. Eng. Chem., Vol. 33 (February, 1941), pp. 249-256.

(11) McMillen, E.L. "Simplified Pressure Loss Calculations for Plastic Flow." Chem. Eng. Prog., Vol. 44 (July, 1948), pp. 537-546.

(12) Thomas, D.G. "Non-Newtonian Suspensions.' Ind. Eng. Chem., Vol. 55 (November, 1963), pp. 18-29.

(13) Wilkinson, W.L. Non-Newtonian Fluid. London: Pergamon Press, 1960.

(14) Skelland, A.H. Non-Newtonian Flow and Heat Transfer. New York: John Wiley and Sons, Inc., 1967.

(15) Eirich, F.R. (Ed.). Rheology - Theory and Applications. New York: Academic Press, 1960.

(16) Atabek, H.B. "Startup Flow of a Bingham Plastic in a Circular Tube." ZAMM, Vol. 44 (1964), pp. 332-333.

(17) Duggins, R.K. "The Commencement of Flow of a Bingham Plastic Fluid," Chemical Engineering Science, Vol. 27 (1972), pp. 1991-1996.

(18) Beaman, J.J. "Transient Velocity Profiles of Bingham Plastics in Circular Pipes." (Unpublished M.S. Thesis, University of Texas, Austin, 1975.)

(19) Meyer, G.H. "A Numerical Method for Two Phase Stefan Problems." SIAM Journal of Numerical Analysis, Vol. 8 (March, 1971), pp. 555-568.

(20) Reid, K.N. "Dynamic Models of Fluid Transmission Lines." Proc. Symposium on Fluids and Internal Flows, Pennsylvania State University, Oct. 24 and 25, 1968, pp. 1-143.

(21) Reid, K.N. "An Analytical and Experimental Study of a Pulsating-flow Hydraulic System." A report submitted to the Allis Chalmers Company Construction Machinery and Form Equipment Div., March 1971.

(22) Kirshner, J.M., and Katz, S. Design Theory of Fluidic Components. Chapter 3, New York: Academic Press, 1975, pp. 63-130.

(23) Brown, F.T. "A Quasi Method of Characteristics with Application to Fluid Lines with Frequency Dependent Wall Shear and Heat Transfer." Journal of Basic Engineering, ASME Trans., Series D, Vol. 93 (June, 1967), pp. 217-226.

(24) Baltzer, R.A. "Column Separation Accompanying Liquid Transients in Pipes." Journal of Basic Engineering, ASME Trans., Series D, Vol. 89 (December, 1967), pp. 837-846.

(25) Streeter, V.L. "Unsteady Flow Calculations by Numerical Methods." Journal of Basic Engineering, ASME Trans., Series D, Vol. 94 (June, 1972), pp. 457-466.

(26) Safwat, H.H., and Van Der Polder, J. "Experimental and Analytic Data Correlation Study of Water Column Separation." Journal of Fluids Eng., ASME Trans., Series I, Vol. 95 (March, 1973), pp. 91-97.

(27) Schweitzer, P.H., and Szebehely, V.C. "Gas Evolution in Liquids and Cavitation." Journal of Applied Physics, Vol. 21 (1950), pp. 1218-1224.

(28) Driels, M.R. "An Investigation of Pressure Transients in a System Containing a Liquid Capable of Air Absorption." Journal of Fluids Engineering, ASME Trans., Series I, Vol. 95 (September, 1973), pp. 408-414.

(29) Brown, R.J. "Water Column Separation at Two Pumping Plants." Journal of Basic Eng., ASME Trans., Vol. 90 (1968), pp. 521-531.

(30) Kranenburg, C. "Gas Release During Transient Cavitation in Pipes." Journal of Hyd. Div., ASCE, Vol. 100 (October, 1974), No. HY10, pp. 1383-1398.

(31) Bird, R.B., Stewart, W.E., and Lightfoot, E.N. Transport Phenomena. New York: John Wiley and Sons, Inc., 1966.

(32) Garabedian, P.R. Partial Differential Equations. New York: John Wiley and Sons, Inc., 3rd Printing, 1967.

(33) Szymanski, F. "Quelques Solutions Exactes des Equations de 1'Hydrodynamique de Fluide Visquex dans le Cas d'un Tube Cylindrique." J. de math. pures et aplliquees, Series 9, Vol. 11 (1932), p. 67.

(34) Trikha, A.K. "An Efficient Method for Simulating Frequency Dependent Friction in Transient Liquid Flow." Transactions of the ASME, Ser. I, Vol. 97 (March, 1975), pp. 97-105.

APPENDIX A

DERIVATIONS RELATED TO THE TIME-DEPENDENT FRICTION MODEL

The following two derivations are related to the time-dependent friction model discussed in Chapter VI.

1. Derivation for $\sum_{m=1}^{\infty} \frac{1}{z_m^2} = \frac{1}{4}$:

The Fourier-Bessel expansion for $1 - \frac{r^2}{R^2}$ is given as

$$1 - \frac{r^2}{R^2} = \sum_{m=1}^{\infty} \frac{8}{z_m^3} \frac{J_0(\frac{r}{R} z_m)}{J_1(z_m)}. \tag{A.1}$$

Differentiating Equation (A.1) with respect to r, gives

$$-\frac{2r}{R^2} = -\sum_{m=1}^{\infty} \frac{8}{z_m^3} (\frac{z_m}{R}) \frac{J_1(\frac{r}{R} z_m)}{J_1(z_m)}. \tag{A.2}$$

After substituting R for r and rearranging, Equation (A.2) becomes

$$\sum_{m=1}^{\infty} \frac{1}{z_m^2} = \frac{1}{4}. \tag{A.3}$$

2. Derivation of error bound on approximating the sum of the infinite series by the sum of a finite series:

$$\text{Let } S = \sum_{m=1}^{\infty} \frac{e^{-pz_m^2}}{z_m^2} \tag{A.4}$$

where $p = \frac{\nu \Delta t}{R^2}$,

$$\text{and let } S_N = \sum_{m=1}^{N} \frac{e^{-pz_m^2}}{z_m^2}. \tag{A.5}$$

If $S - S_N$ gives the error between the sums, then

$$S - S_N = \sum_{m=N+1}^{\infty} \frac{e^{-pz_m^2}}{z_m^2}. \tag{A.6}$$

Since the zeros of the Bessel function $J_0(x)$ form a monotonically increasing sequence,

$$S - S_N < e^{-pz_{N+1}^2} \sum_{m=N+1}^{\infty} \frac{1}{z_m^2}. \tag{A.7}$$

Using Equation (A.3), Equation (A.7) can be rewritten as

$$S - S_N < e^{-pz_{N+1}^2} \left(\frac{1}{4} - \sum_{m=1}^{N} \frac{1}{z_m^2}\right) \tag{A.8}$$

Equation (A.8) indicates the error bound in using a finite number of zeros of the Bessel function $J_0(x)$ in the evaluation of τ_w using Equation (4.44).

APPENDIX B

PROGRAM LISTINGS

```
C     THE FOLLOWING PROGRAMS ARE BASED ON THE MODELS DEVELOPED IN
C     CHAPTERS IV AND V. THE MAIN PROGRAM READS INPUT PARAMETER VALUES,
C     CALLS SUBROUTINE LINEO FOR EVERY TIME STEP, AND WRITES THE OUTPUT
C     PRESSURES AT DIFFERENT GRID POINTS (ARRAY PA) TO THE DISK FILE
C     WHICH IS USED LATER TO OBTAIN THE PLOTS. THE MAIN PROGRAM CALLS
C     THE FOLLOWING SUBROUTINES:
C           1. SUBROUTINE LINEO
C           2. SUBROUTINE PQDMP
C     SUBROUTINE PQDMP IS CALLED ONLY IF A DUMP OF ALL THE PRESSURE
C     AND FLOW VARIABLES IS NEEDED. THE LISTING OF SUBROUTINE PQDMP IS
C     NOT PROVIDED.
C     THE LOGICAL UNITS AND THEIR USES ARE LISTED BELOW:
C     LU 5  - INPUT LOGICAL UNIT TO READ THE PARAMETER VALUES.
C     LU 6  - OUTPUT LOGICAL UNIT TO PRINT THE OUTPUT.
C     LU 8  - OUTPUT LOGICAL UNIT TO STORE PLOT DATA.
C     LU 10 - OUTPUT LOGICAL UNIT TO DUMP THE VARIABLE VALUES (USED BY
C             PQDMP).
C     A COMPLETE GLOSSARY OF THE VARIABLES IS NOT PROVIDED. ONLY THOSE
C     VARIABLES THAT NEED SOME EXPLANATION ARE GIVEN BELOW:
C     EVTC  - TIME CONSTANT FOR AIR RELEASE (TC)
C     MU    - COEFFICIENT OF PLASTICITY
C     NORFC - FLAG TO CHOOSE LINEARIZED OR NON-LINEARIZED ORIFICE
C           - 0 LINEAR ORIFICE MODEL FOR UPSTREAM AND DOWNSTREAM ENDS
C           - 1 LINEAR ORIFICE MODEL FOR UPSTREAM AND NON-LINEAR
C               ORIFICE AT THE DOWNSTREAM END
C           - 2 NON-LINEAR ORIFICE MODEL FOR BOTH ENDS
C     INPMOD - FLAG TO CONTROL INPUT MODE
C            - 0 INITIAL STEADY-STATE INPUT IS PRESSURE
C            - 1 INITIAL STEADY-STATE INPUT IS FLOW RATE
C     RNTCL  - VALVE CLOSURE TIME
C     QS     - INITIAL STEADY-STATE FLOW RATE
C     PINIT  - INITIAL STEADY-STATE PRESSURE
C     RKS    - SOLUBILITY CONSTANT FOR THE LIQUID
C     TAFT   - TIME AT WHICH DOWNSTREAM VALVE BEGINS TO CLOSE OR OPEN
C
      IMPLICIT REAL*8(A-H,O-Z)
      COMMON/NALL/Y(1),DY(1),X(220),P(50),TIME,BEGTIM,
     1          ENDTIM,DELT
      COMMON /OUTPUT/PA(300)
      COMMON /ORFCE/CDS,CDL
C
      COMMON /AIRREL/ALPHA,ALPHI
C
      COMMON /FLAGS/IBOUT,IRUN,ISTART,ISTOPU,IDUMP
C
      COMMON /MISC/PI,NSUBK,MODE
C
      DIMENSION ICOM(20),IXL(9),IYL(9),RLEN(5),H(5)
      DIMENSION IYL1(9)
C
      REAL*4 PA,TME,SNGL
      REAL*8 MU,L,NSUBK
C
      EQUIVALENCE    (X(10),PIN),      (X(111),POUT)
C
      EQUIVALENCE (P(1),RNTCS),            (P(2),RNTCL),
     *            (P(3),NPSEG),           (P(4),G),
     *            (P(5),VP),           (P(10),NGRIDS)
```

```
     *            (P(6),MU),                (P(7),RHO),
     1          (P(8),BETA),               (P(9),TAUO),
     2           (P(11),L),                 (P(12),D),
     3            (P(13),RNDO),              (P(14),DL),
     4           (P(15),RL),                (P(16),DSOURS),
     5           (P(17),RLS),               (P(18),TAFTO),
     6            (P(19),TAFT),              (P(20),ERROR),
     7           (P(21),INPMOD),             (P(22),TURNON),
     8            (P(23),TURNOF),            (P(24),DELTAT),
     9            (P(25),TWERR),             (P(26),ITWMOD),
     1            (P(27),PF),                (P(28),QF),
     1           (P(29),PINIT),
     2            (P(30),RLEN(1)),           (P(35),H(1)),
     3            (P(40),BEGTMD),            (P(41),ENDTMD),
     4            (P(42),NGRD1),             (P(43),NGRD2),
     5            (P(44),IEXACT),            (P(45),R)
      EQUIVALENCE (P(46),RKS),               (P(47),EVTC),
     1            (P(48),NZERO),                (P(49),PSAT),
     2            (P(50),NORFC)
C
C
      NAMELIST /DATA/Y,X,P,TIME,BEGTIM,ENDTIM,DELT,
     1   MU,RHO,BETA,TAUO,L,D,RNDO,PF,NSKIP,DL,RL,TAFT,PIN,DSOURS,RLS,
     2   TAFTO,QS,ERROR,INPMOD,TURNON,TURNOF,DELTAT,TWERR,ITWMOD,RLEN,
     3   H,G,NPSEG,PINIT,VP,BEGTMD,ENDTMD,NGRD1,NGRD2,IDUMP,LUDMP,RNTCS,
     4 RNTCL,IEXACT,R,RKS,EVTC,NZERO,PSAT,NGRIDS,IEXP,NORFC,CDS,CDL,
     5 DP1,DP2,ALPHA,ALPHI
      NAMELIST /DTAOUT/TIME,BEGTIM,ENDTIM,DELT,MU,RHO,BETA,TAUO,D,
     1  RNDO,PF,QF,NSKIP,DL,RL,TAFT,PIN,QS,ERROR,DSOURS,RLS,TAFTO,
     2 INPMOD,TURNON,TURNOF,DELTAT,TWERR,ITWMOD,NPSEG,G,VP,RLEN,H,PINIT,
     3 IDUMP,BEGTMD,ENDTMD,NGRD1,NGRD2,RNTCS,RNTCL,IEXACT,R,RKS,EVTC,
     4 PSAT,NGRIDS,IEXP,NZERO,DP1,DP2,NORFC,CDS,CDL,ALPHA,ALPHI
C
      DATA LUDMP/10/
C
      ATAN(X)=DATAN(X)
C
C
C     SET THE DEFAULT VALUES ***
C
      ALPHA=0.1
      IEXP=0
      RKS=0.0184
      EVTC=0.1795
      NZERO=60
      PSAT=0.0
      IDUMP=0
      NGRIDS=0
      NGRD1=1
      NGRD2=1
      BEGTMD=0.0
      ENDTMD=0.0
      NPSEG=1
      G=386.0
      VP=-14.24
      RLEN(1)=1200.0
      H(1)=0.0
      PINIT=0.0
```

```
      REWIND 10
      PIN=0.0
      TWERR=1.0D-6
      ITWMOD=1
      PI=ATAN(1.D0)*4.D0
      NR=5
      BEGTIM=0.0
      ENDTIM=2.0
      DELT=1.0D-4
      NSKIP=10
      IND=1
      IX=1
      MU=20.0*0.145E-6
      RHO=76.0/32.2/(12.0**4)
      BETA=2.0D5
      TAU0=2.9D-4
      DELTAT=0.4*TAU0
      RNDO=2.0
      PF=10.0
      L=1200.0
      D=1.0
      DL=.25
      DSOURS=.25
      RL=6.0
      RL8=6.0
      TAFT=9.0
      TAFT0=3.0
      ERROR=.5D-4
      QS=.5
      INPMOD=0
      TURNON=0.0
      TURNOF=10.0
      DP1=144.0
      DP2=72.0
C
C     READ THE DATA ***
C
   60 READ(NR,DATA,END=100)
      L=0.0
      DO 110 I=1,NPSEG
110   L=L+RLEN(I)
      QF=PF*PI*D**4/(128.0*MU*L)
      IF (INPMOD.EQ.0) GO TO 65
      PINIT=QS/QF
65    CONTINUE
C
C     PRINT THE PARAMETER VALUES USED FOR SIMULATION.
C
      TIME=BEGTIM
      WRITE(6,DTAOUT)
      I=0
      II=1
C
C     ESTABLISH INITIAL STEADY-STATE CONDITIONS.
C
      MODE=0
      TIME=BEGTIM-DELT
      CALL LINEQ(NGRIDZ)
```

```
      TIME=BEGTIN
      MP=NGRIDZ/2+1
      CALL PQUMP(LUUMP)
      TME=SNGL(TIME)
      NGW=NGRIDZ
C
C     ESTABLISH THE GRID POINTS THAT CORRESPOND TO THE PRESSURE TRANS-
C     DUCER POSITIONS IN THE EXPERIMENTAL SETUP.
C
      IF (IEXP.NE.1) GO TO 200
      TEMP1=FLOAT(NGRIDZ)+0.5
      NP1=IFIX(SNGL(TEMP1-DP1*(NGRIDZ-1)/L))
      NP2=IFIX(SNGL(TEMP1-DP2*(NGRIDZ-1)/L))
      NGW=NGRIDZ+4
      WRITE (6,67) NGW,NP1,NP2
67    FORMAT(/1X,'NGW= ',I4,2X,'NP1= ',I4,2X,'NP2= ',I4)
C
C     STORE THE NO. OF GRIDS, THE INITIAL STARTING TIME, AND THE
C     CORRESPONDING PRESSURE DISTRIBUTION ON UNIT 8.
C
200   WRITE (8) NGW
      WRITE(8) TME,(PA(IW), IW=1,NGRIDZ,2),
     1 PA(NP2),PA(NP1)
C
C     PRINT THE STARTING TIME AND FLOW RATES AT THE UPSTREAM AND
C     DOWNSTREAM ENDS OF THE PIPELINE.
C
      TME=SNGL(TIME)
      QNG=SNGL(X(111+NGRIDZ))*QF
      Q1=SNGL(X(112))*QF
      WRITE (6,2000)
2000  FORMAT(/6X,'TIME',14X,'Q1',15X,'QNG'/)
      WRITE (6,*) TME,Q1,QNG
C
C     EVALUATE AND WRITE THE VALUES OF PRESSURE AND FLOW RATES TO
C     APPROPRIATE LOGICAL UNITS AT EVERY TIME STEP.
C
50    MODE=1
      TIME=TIME+DELT
      CALL LINEO(NGRID7)
      CALL PQUMP(LUUMP)
      TME=SNGL(TIME)
      WRITE (8) TME,(PA(IW), IW=1,NGRIDZ,2),
     1 PA(NP2),PA(NP1)
      I=I+1
      IF (MOD(I,NSKIP).NE.0) GO TO 70
      II=II+1
      Q1=SNGL(X(112))*QF
      QNG=SNGL(X(213))
      WRITE(6,*)TME,Q1,QNG
   70 IF(TIME.LT.(ENDTIM-DELT)) GO TO 50
      GO TO 60
  100 CONTINUE
      REWIND 8
      REWIND 10
      STOP
      END
```

```
      SUBROUTINE TAUWEV(QP,TAUUP)
C
C     THIS SUBROUTINE EVALUATES THE WALL SHEAR STRESS IN THE LAMINAR
C     AND TURBULENT FLOW REGIMES BASED ON STEADY-STATE FRICTION.
C
      IMPLICIT REAL*8 (A-H,O-Z)
      COMMON /WALL/Y(1),DY(1),X(220),P(50),TIME,BEGTIM,
     1            ENDTIM,DELT
C
      COMMON /FLAGS/IBOUT,IRUN,ISTART,ISTOPU,IDUMP
C
      COMMON /MISC/PI,NSUBK,MODE
C
      REAL*8 MU,L,MUO,NSUBK,MUOO
C
      EQUIVALENCE     (X(10),PIN)
C
      EQUIVALENCE (P(3),NPSEG),              (P(4),G),
     *            (P(5),VP),
     *            (P(6),MU),                 (P(7),RHO),
     1          (P(8),BETA),                (P(9),TAUO),
     2           (P(11),L),                  (P(12),D),
     3            (P(13),RNDO),               (P(14),DL),
     4           (P(15),RL),                 (P(16),DSOURS),
     5           (P(17),RLS),                (P(18),TAFTO),
     6            (P(19),TAFT),               (P(20),ERROR),
     7            (P(21),INPMOD),              (P(22),TURNON),
     8             (P(23),TURNOF),             (P(24),DELTAT),
     9             (P(25),TWERR),              (P(26),ITWMOD),
     1             (P(27),PF),                 (P(28),QF),
     2             (P(44),IEXACT)
C
      DATA IST/0/
C
C
      ABS(X)=DABS(X)
      SIGN(X,Y)=DSIGN(X,Y)
      ALOG10(X)=DLOG10(X)
C
      IF (IST.NE.0) GO TO 200
      IST=1
C
C     PERFORM THE INITIAL CALCULATIONS TO EVALUATE THE CONSTANTS.
C
100   TAU1=TAUO+DELTAT
      TAUOP=TAUO/PF
      TAUO43=4.0*TAUO/3.0
      PIR3=PI*(D/2.0)**3
      REC1=4.0*RHO*QF/(PI*MU*D*3.0)
      REC2=8.0*RHO*QF*QF/(PI**2*D**4*PF)
      RLNR=0.25*D/L
      IF (ITWMOD.EQ.1) GO TO 110
      TAUOB3=TAUO/3.0
      MUO=MU*TAU1/(TAU1-TAUO43+TAUOB3*(TAUO/TAU1)**3)
      RLNRMO=0.25*(MUO/MU)*D/L
      QOP=TAU1/(RLNRMO*PI)
      ASSIGN 220 TO IGOTO
      GO TO 900
```

```
110   IF (TAU1.LE.TAU043) GO TO 120
      MU0=MU*TAU1/(TAU1-TAU043)
      RLNRM0=0.25*(MU0/MU)*D/L
      QOP=TAU1/(RLNRM0*PF)
      ASSIGN 230 TO IGOTO
900   WRITE(6,*) MU0
      GO TO 1000
120   WRITE(6,130)
130   FORMAT(1X,'** ERROR ** TAU1 IS LESS THAN TAU0*1.3333')
      STOP 10
C
C     EVALUATE THE WALL SHEAR STRESS BASED ON THE STEADY-STATE FRICTION
C     IN THE LAMINAR FLOW CASE.
C
200   IF (TIME.GE.BEGTIM.AND.IEXACT.EQ.1) GO TO 1010
      IF (ABS(QP).GE.QOP) GO TO 210
      TAUWP=RLNRM0*QP
      GO TO 1000
210   SIGNQ=SIGN(1.0D0,QP)
      GO TO IGOTO,(220,230)
220   A=TAU043/PF*SIGNQ+RLNR*QP
      TWOLD=A
240   TWNEW=A-TAU0B3*(TAU0P/TWOLD)**3/PF
      IF (ABS(TWNEW-TWOLD).LE.TWERR) GO TO 250
      TWOLD=TWNEW
      GO TO 240
250   TAUWP=TWNEW
      GO TO 500
230   TAUWP=TAU043/PF*SIGNQ+RLNR*QP
500   C=ABS(TAU0P/TAUWP)
      RE=REC1*ABS(QP)*(1.-C)*(C**4-4.*C+3.0)
      IF (RE.LT.2000) GO TO 1000
C
C     IF NR > 2000 EVALUATE THE WALL SHEAR STRESS USING TOMITA'S
C     CORRELATIONS IN THE TURBULENT FLOW CASE.
C
      XOLD=1.0
      ITER=0
      TEMP=4.0*ALOG10(RE)-0.4
510   XNEW=1.0/(TEMP+4.0*ALOG10(XOLD))
      ITER=ITER+1
      IF (ABS(XNEW-XOLD).LT.0.01*XNEW) GO TO 520
      IF (ITER.GE.100) GO TO 2000
      XOLD=XNEW
      GO TO 510
520   FRICF=XNEW**2
      TAUWP=REC2*FRICF*QP*QP*SIGNQ
300   CONTINUE
1000  RETURN
1010  TAUWP=0.0
      RETURN
2000  WRITE(6,2010)
2010  FORMAT(1X,'** ERROR ** NO. OF ITERATIONS EXCEEDED 100 ',
     1 'FOR FRICTION FACTOR EVALUATION'/)
      STOP 2010
      ENTRY FINDM0(MU00,TAU1P)
      MU00=MU0
      TAU1P=TAU1/PF
      RETURN
      END
```

```
      SUBROUTINE  PTAUWE (NGNOW,ITIME,NGRID,CONST2,TAUWP)
C
C     THE FOLLOWING SUBROUTINE IS USED BY SUBROUTINE LINEO
C     TO EVALUATE THE WALL SHEAR STRESS BASED ON THE TIME-DEPENDENT
C     FRICTION.
C
C
      IMPLICIT REAL*8 (A-H,O-Z)
      COMMON/NALL/Y(1),DY(1),X(220),P(50),TIME,BEGTIM,
     1           ENDTIM,DELT
C
      COMMON /FLAGS/IHOUT,IRUN,ISTART,ISTOPU,IDUMP
      COMMON /MISC/PI,NSUBK,MODE
C
      REAL*8 MU,L,MUO,NSUBK
C
      DIMENSION PP(101), TWM(61,101),WM(60,4)
C
      EQUIVALENCE (X(10),PIN)
      EQUIVALENCE (X(11),PP(1))
      EQUIVALENCE (P(3),NPSEG),              (P(4),G),
     *            (P(5),VP),
     *            (P(6),MU),                 (P(7),RHO),
     1          (P(8),BETA),                (P(9),TAUO),
     2           (P(11),L),                  (P(12),D),
     3            (P(13),RNDO),               (P(14),DL),
     4           (P(15),RL),                 (P(16),DSOURS),
     5           (P(17),RLS),               (P(18),TAFTO),
     6            (P(19),TAFT),               (P(20),ERROR),
     7            (P(21),INPMOD),              (P(22),TURNON),
     8             (P(23),TURNOF),              (P(24),DELTAT),
     9             (P(25),TWERR),               (P(26),ITWMOD),
     1             (P(27),PF),                  (P(28),QF),
     1           (P(29),PINIT),                    (P(48),NZERO)
C
C
      SQRT(X)=DSQRT(X)
      ABS(X)=DABS(X)
C
C
      IF (MODE.NE.0) GO TO 50
C
C     PERFORM THE INITIAL CALCULATIONS FOR THE CONSTANTS.
C
      DELTIM=DELT/RNDO
      DELTB2=DELTIM/2.0
      CALL FINDMO(MUO,TAUIP)
      NGRIDZ=NGRID
      C2M1=4.0*MU/(RHO*D*D)
      WRITE (6,25) MUO,MU,TAUIP
25    FORMAT(1X,'MUO = ',G11.4,' MU = ',G11.4,' TAUIP = ',G11.4)
      C2M2=C2M1*MUO/MU
      CONST=CONST2
      DELTZ2=2.0*L/(NGRIDZ-1)
      TMEP=DELTB2*C2M1
      DO 20 I=1,NZERO
      WM(I,1)=W(TMEP,I)
20    WM(I,2)=W1(WM(I,1),I)
      TMEP=DELTB2*C2M2
      DO 30 I=1,NZERO
      WM(I,3)=W(TMEP,1)
30    WM(I,4)=W1(WM(I,3),I)
      PGRADS=(PP(1)-PP(3))/DELTZ2*D
      DO 40 I=1,NZERO
```

```
      WTEMP=W1(PGRADS,I)
      DO 40 J=1,NGRID
40    TWM(1,J)=WTEMP
      NZERO1=NZERO+1
      DO 45 J=1,NGRID
45    TWM(NZERO1,J)=PGRADS*0.25
      GO TO 1000
50    CONTINUE
C
C     EVALUATE WALL SHEAR STRESS BASED ON THE TIME-DEPENDENT FRICTION
C     AT A GIVEN GRID POINT.
C
      SUM=0.0
      M=1
      IF (ABS(TWM(NZERO1,NGNOW)).LT.TAU1P) M=3
      IF (NGNOW.EQ.1) GO TO 230
      IF (NGNOW.EQ.NGRIDZ) GO TO 240
      PGRAD=D*(PP(NGNOW-1)-PP(NGNOW+1))/DELTZ2
      GO TO 220
230   PGRAD=D*(PP(1)-PP(2))*2.0/DELTZ2
      GO TO 220
240   PGRAD=D*(PP(NGRIDZ-1)-PP(NGRIDZ))*2.0/DELTZ2
220   SUM=0.0
      CALL ERRSET(208,256,2,1)
      DO 250 I=1,NZERO
      TWM(I,NGNOW)=TWM(I,NGNOW)*WM(I,M)+W1(PGRAD,I)-PGRAD*WM(I,M+1)
250   SUM=SUM+TWM(I,NGNOW)
      CALL ERRSET(208,10,10,2)
      TWM(NZERO1,NGNOW)=SUM
      TAUWP=SUM*CONST
1000  RETURN
      END
      DOUBLE PRECISION FUNCTION W(TMEP,I)
C     THIS FUNCTION SUBPROGRAM IS USED BY THE SUBROUTINE PTAUWE
C     TO EVALUATE THE EXPONENTIAL TERM IN EQUATION 4.46 OF THE TEXT.
C
C
      IMPLICIT REAL*8 (A-H,O-Z)
      COMMON/NALL/Y(1),DY(1),X(220),P(50),TIME,BEGTIM,
     1            ENDTIM,DELT
CC
      COMMON /OUTPUT/XX(300),YY(300),ZZ(300),PA(300),PM(300)
C
      COMMON /FLAGS/IBOUT,IRUN,ISTART,ISTOPU,IDUMP
C
      REAL MU
      DIMENSION ZEROS2(61)
C
      EQUIVALENCE (P(3),NPSEG),              (P(4),G),
     *            (P(5),VP),
     *            (P(6),MU),                 (P(7),RHO),
     1          (P(8),BETA),                (P(9),TAU0),
     2           (P(11),L),                  (P(12),D),
     3            (P(13),RND0),                (P(14),DL),
     4           (P(15),RL),                 (P(16),DSOURS),
     5           (P(17),RLS),                (P(18),TAFT0),
     6            (P(19),TAFT),               (P(20),ERROR),
     7            (P(21),INPMOD),              (P(22),TURNON),
     8             (P(23),TURNOF),              (P(24),DELTAT),
     9             (P(25),TWERR),               (P(26),ITWMOD),
     1             (P(27),PF),                  (P(28),QF),
     1           (P(29),PINIT),                    (P(40),NZERO)
      DATA MODE1/0/
C
C     ZEROS OF THE BESSEL FUNCTION JO(X)
C
```

```
      DATA ZEROS2/5.7831D0,30.4715D0,74.8865D0,139.039D0,222.9318D0,
     1326.5647D0,449.932D0,593.0443D0,755.8925D0,938.4787D0,
     21140.805D0,1362.872D0,1604.6754D0,1866.22D0,2147.5068D0,2448.528D0
     3,2769.29ED0,3109.791D0,3470.035D0,3850.016D0,4249.736D0,4669.1938D
     40,5108.389ZD0,5567.3231D0,6045.9955D0,6544.4216D0,7062.5703D0,
     57600.457D0,8158.0998D0,8735.4632D0,9332.5039D0,9949.4241D0,
     610586.022D0,11242.339D0,11918.416D0,12614.232D0,13329.764D0,
     714065.058D0,14820.067D0,15594.839D0,16389.35D0,17203.575D0,
     818037.564D0,18891.292D0,19764.76D0,20657.939D0,21570.885D0,
     922503.57D0,23455.994D0,24428.127D0,25420.029D0,26431.67D0,
     127463.052D0,28514.138D0,29584.997D0,30675.595D0,31785.933D0,
     232916.01D0,34065.789D0,35235.344D0,36666.66D0/
C
      ABS(X)=DABS(X)
      EXP(X)=DEXP(X)
      SQRT(X)=DSQRT(X)
C
      IF (MODE1.NE.0) GO TO 10
      MODE1=1
      SUM=0.0
      DO 20 J=1,NZERO
20    SUM=SUM+1.0/ZEROS2(J)
      ERRORS=EXP(-TMEP*ZEROS2(NZERO+1))*(0.25-SUM)
      WRITE (6,30) ERRORS,ZEROS2(NZERO+1)
30    FORMAT(1X,'ERROR IN SUM',2D12.4)
10    W=EXP(-ZEROS2(I)*TMEP)
      RETURN
      ENTRY W1(WTEMP,I)
      W1=WTEMP/ZEROS2(I)
      RETURN
      END
```

```
C     THE FOLLOWING SUBROUTINE LINEO IMPLEMENTS THE METHOD OF
C     CHARACTERISTICS SOLUTION TECHNIQUE ALONG WITH THE LINE MODELS
C     DEVELOPED IN CHAPTER IV AND V.
C     THE SUBROUTINES ORFC,ORFCO,QUADS,QUADL CALLED BY THIS ROUTINE ARE
C     NOT LISTED SINCE THEY IMPLEMENT ONLY THE ORIFICE MODELS AT
C     UPSTREAM AND DOWNSTREAM ENDS. SUBROUTINE ZXGSP IS AN IMSL ROUTINE.
C     A DETAILED DESCRIPTION OF IT CAN BE FOUND IN CHAPTER Z, VOL.3 OF
C     THE IMSL PROGRAM DOCUMENTATION.
C
      SUBROUTINE LINEO(NGRIDZ)
      IMPLICIT REAL*8(A-H,O-Z)
      EXTERNAL      F
      COMMON/NALL/Y(1),DY(1),X(220),P(50),TIME,BEGTIM,
     1           ENDTIM,DELT
CC
      COMMON /OUTPUT/PA(300)
C
      COMMON /FLAGS/IBOUT,IRUN,ISTART,ISTOPU,IDUMP
C
      COMMON /MISC/PI,NSUBK,MODE
      REAL*4 PA
      REAL*8 DSUBK,MU,L
      DIMENSION TEMPP(101),TEMPQ(101)
C
      COMMON /SOLVER / ORL(101),PAR1(8),
     1 OMINUS(101),DELTMP,CRATIO,TPP1,TPM1,TQM1,ICAV(101)
      COMMON /AIREL/ALPHA,ALPHI
C
      DIMENSION DELH(5),RLEN(5),H(5),VCAV(101),VOLA(101),RMT(101)
C
C*****************************************************************
C     FOR INITIAL STEADY-STATE ANALYSIS;
      DIMENSION PAR(10)
C
C*****************************************************************
      EQUIVALENCE  (X(11),TEMPP(1)),   (X(112),TEMPQ(1)),
     1         (X(10),PIN),        (X(213),QOUT)
      EQUIVALENCE      (X(111),POUT)
C
      EQUIVALENCE (P(3),NPSEG),              (P(4),G),
     *            (P(5),VP),
     *            (P(6),MU),                 (P(7),RHO),
     1          (P(8),BETA),                (P(9),TAUO),
     1          (P(10),NGRIDS),
     2           (P(11),L),                  (P(12),D),
     3            (P(13),RNDO),                (P(14),DL),
     4           (P(15),RL),                 (P(16),DSOURS),
     5           (P(17),RLS),                (P(18),TAFTO),
     6            (P(19),TAFT),               (P(20),ERROR),
     7            (P(21),INFMOD),              (P(22),TURNON),
     8             (P(23),TURNOF),              (P(24),DELTAT),
     9             (P(25),TWERR),               (P(26),ITWMOD),
     1             (P(27),PF),                  (P(28),QF),
     1           (P(29),PINIT),
     2             (P(30),RLEN(1)),             (P(35),H(1)),
     3             (P(44),IEXACT),               (P(45),R),
     4             (P(46),RKS),                  (P(47),EVTC),
     5             (P(48),NZERO),                   (P(49),PSAT),
```

```
     6            (P(40),BEGTMD),              (P(41),ENDTMD)
      EQUIVALENCE (P(50),NORFC)
C
C
      SQRT(X)=DSQRT(X)
      SIGN(X,Y)=DSIGN(X,Y)
      ABS(X)=DABS(X)
      FLOAT(K)=DFLOAT(K)
      EXP(X)=DEXP(X)
      ASIN(X)=DARSIN(X)
      SIN(X)=DSIN(X)
C
      IF (MODE-1) 100,200,300
C
C
C
C     INITIALIZATION ***
C
100   AF=SQRT(BETA/RHO)
      DELTIM=DELTIM/RNDO
      RG=RHO*G/PF
      VP=VP/PF
      DELTMP=DELTIM*AF/L
      NGRIDZ=NGRIDS
      IF (NGRIDS.EQ.0)
     1 NGRIDZ=IFIX(1.0/SNGL(DELTMP)+0.5)*2+1
      AREA=PI*R**2/4.0
      NSUBE=SQRT(RHO*BETA)*AREA/(8.0*PI*MU*L)
      DELZB2=1./(NGRIDZ-1)
      DELTZ=DELZB2+DELZB2
      CRATIO=0.0
      IF (NGRIDS.NE.0)
     1 CRATIO=(1.0-DELTIM*0.5*AF/DELZB2)*0.5
      VL=DELZB2*AREA
      CONST3=(1.0-EXP(-DELTIM*EVTC))
      VOLREF=L*QF/AF
      VOLAM=RNSPVL*((PSAT+14.7)/(VP+14.7)-1.0)
      VOLAM=VOLAM/VOLREF
      PHTWP=0.0
      DELH(1)=RG*H(1)*DELZB2/RLEN(1)
      IF (NPSEG.LE.1) GO TO 130
      DO 120 I=2,NPSEG
120   DELH(I)=RG*(H(I)-H(I-1))*DELZB2/RLEN(I)
130   NRO=IFIX(SNGL(RNDO)+0.5)
      ITIME=0
      PIMP=PSOURC(DUMMY)/PF
      CALL FACWEV(DUMMY,DUMMY)
      IFLTMP=NORFC
      NORFC=0
      CALL ORFCO(RSOURC)
      CALL ORFC(RLOAD)
      NORFC=IFLTMP
      IF (NORFC.EQ.2) CALL ORFCO(CS)
      IF (NORFC.GE.1) CALL ORFC(CL)
C
C*********************************************************************
C
C     FIND THE STEADY-STATE FLOW AND INITIALIZE THE GRIDS
```

```
C     ACCORDINGLY.
C
      PEP=RG*R(NPSEG)
      IF (IOPMOD.EQ.1) GO TO 111
      PSTP=PSOURC(DUMMY)/PF
      RLINE=1.0
      PD=PSTP-PEP
      QAPP=PD/(RSOURC+RLOAD+RLINE)
      IF (QAPP.NE.0.0) GO TO 105
      WRITE (6,1030) QAPP
      QINS=0.0
      GO TO 110
105   PAR(1)=PD
      PAR(4)=L
      PAR(5)=D
      TOL=ERROR*ABS(QAPP)
      IF(NORFC.GE.2) GO TO 106
      PAR(2)=RSOURC
      PAR(3)=RLOAD
      IF (NORFC.EQ.1) PAR(3)=CL
      GO TO 107
106   PAR(2)=CS
      PAR(3)=CL
107   CALL ZXGSP(F,PAR,PDUM,IDUM,1,1,0.,2.*QAPP,TOL,
     1 QINS,ILR)
110   IF (NORFC.EQ.0) PDL=PD-QINS*(RSOURC+RLOAD)
      IF (NORFC.EQ.2) PDL=PD-ABS(QINS)*QINS*(1/CS**2+1/CL**2)
      IF (NORFC.EQ.1) PDL=PD-RSOURC*QINS-ABS(QINS)*QINS/CL**2
      GO TO 112
111   QSP=QINIT
      CALL TAUSEV(QSP,TWS)
      QINS=QSP
      PDL=4.0*TWS*L/D
      IF (NORFC.EQ.0) PD=PDL+QINS*(RSOURC+RLOAD)
      IF (NORFC.EQ.2) PD=PDL+ABS(QINS)*QINS*(1/CS**2+1/CL**2)
      IF (NORFC.EQ.1) PD=PDL+RSOURC*QINS+QINS*ABS(QINS)/CL**2
      PSTP=PD+PEP
      PINIT=PSTP*PF
112   DELP=PDL*DELZ82/L
      IF (NORFC.LE.1) PBEG=PSTP-QINS*RSOURC
      IF (NORFC.EQ.2) PBEG=PSTP-ABS(QINS)*QINS/CS**2
      DO 150 I=1,NGRIDZ
      TEMPP(I)=PBEG-(I-1)*DELP
150   TEMPQ(I)=QINS
C
C*********************************************************************
      DO  160 I=1,101
      VCAV(I)=0.0
      VOLA(I)=0.0
      ICAV(I)=0
      QFI(I)=0.0
160   OMINUS(I)=0.0
      TIME=BUGTIM
      DPINP=(PSOURC(DUMMY)-PINIT)/PF
      IF (NORFC.LE.1) DELQP=DPINP/(NSUBK+RSOURC)
      IF (NORFC.EQ.2.AND.ABS(DPINP).GT.1.0E-9) GO TO 1060
      TEMPQ(1)  DELQP+TEMPQ(1)
      TEMPP(1)=DELQP*NSUBK+TEMPP(1)
```

```
      CONST2=2.0*L/D*DELTMP
      VPAP=ALPHA*(VP+14.7)/PF
      IF (IEXACT.NE.0) CALL PTAUWE (NGNOW,ITIME,NGRIDZ,CONST2,PHTWP)
      WRITE (6,115) NGRIDZ,NDO,NSUBK,AF,QF,PF,TEMPQ(1),TEMPP(1),CRATIO
115   FORMAT (5X,'NO. OF GRIDS = ',I3,/5X,'NDO = ',I2,2X,'NSUBK = ',
     1 G12.5,2X,'AF = ',G12.5,2X,'QF = ',G12.5,2X,'PF = ',G12.5/
     2 5X,'QP1 = ',G12.5,2X,'PP1 = ',G12.5,2X,'CRATIO= ',G12.5)
      WRITE (6,118) RSOURC,RLOAD,CS,CL
118   FORMAT(1X,'RSOURCE= ',G12.5,' RLOAD= ',G12.5,' CS= ',G12.5,
     1 ' CL= ',G12.5/)
      NG=NGRIDZ-1
C
C     SAVE THE INITIAL  VALUES OF PRESSURES.
C
      DO 190 I=2,NPSEG
190   RLEN(I)=RLEN(I-1)+RLEN(I)
      ACCL=0.0
      HADD=0.0
      ISTOP=0
      Z=DELZB2
      IBEG=1
      QOUT=TEMPQ(NGRIDZ)*QF
      PA(1)=TEMPP(1)*PF
      DO 165 I=2,NGRIDZ
      DO 170 IF=IBEG,NPSEG
      IF (Z.LE.RLEN(IF)) GO TO 180
170   CONTINUE
180   IBEG=IF
      IF (IF.NE.1) ACCL=RLEN(IF-1)
      IF (IF.NE.1) HADD=H(IF-1)
      GTZ=(Z-ACCL)*DELH(IF)/DELZB2+HADD*RG
      Z=Z+DELZB2
      PA(I)=(TEMPP(I)-GTZ)*PF
      IF (PA(I).LE.VP) ISTOP=1
165   CONTINUE
      IF (ISTOP.EQ.1) GO TO 185
      GO TO 1000
185   WRITE (6,188) (PA(IW), IW=1,NGRIDZ)
188   FORMAT (/(8(2X,E12.5)))
      STOP 100
C
C     INCREMENT THE VARIABLES FOR ONE TIME STEP ***
C
 200  PINP=PSOURC(DUMMY)/PF
      IBEG=2
      ASSIGN 222 TO ISKIP
      DO 250 INAIN=1,NDO
      Z=DELZB2
      IBEGP=1
 260  DO 220 I=IBEG,NG,2
      QPLUS=TEMPQ(I-1)
      IF (ICAV(I-1).GT.0) QPLUS=QMINUS(I-1)
      TQP1=QPLUS*(1.0-CRATIO)+TEMPQ(I+1)*CRATIO
      TQM1=QPLUS*CRATIO+TEMPQ(I+1)*(1.0-CRATIO)
C
C     EVALUATE WALL SHEAR STRESS BASED ON THE CONSTANT FRICTION MODEL.
C
      CALL TAUWEV(TQP1,TWL)
```

```
      CALL TAUWEV(TQM1,TWR)
C
C     EVALUATE WALL SHEAR STRESS BASED ON THE TIME DEPENDENT FRICTION
C     MODEL.
C
      IF (IEXACT.NE.0) CALL PTAUWE (I,ITIME,NG,CONST2,PHTWP)
      DO 205 IF=IBEGP,NPSEG
      IF (Z.LE.RLEN(IF)) GO TO 206
205   CONTINUE
      GO TO 1010
206   IBEGP=IF
      HADD=0.0
      ACCL=0.0
      IF (IF.NE.1) ACCL=RLEN(IF-1)
      IF (IF.NE.1)HADD=H(IF-1)
      GTZ=(Z-ACCL)*DELH(IF)/DELZR2+HADD*RG
      TPP1=TEMPP(I-1)*(1.0-CRATIO)+TEMPP(I+1)*CRATIO
      TPM1=TEMPP(I-1)*CRATIO+TEMPP(I+1)*(1.0-CRATIO)
      VPP=VPDELTZ
      IF (ICAV(I).GT.0) GO TO 215
      TEMPP(I)=0.5*(TPP1+TPM1+(TQP1-TQM1)*
     1 NSUBK-CONST2*(TWL-TWR))
      TEMPQ(I)=0.5*(TPP1-TPM1+(TQP1+TQM1)*NSUBK
     1 -CONST2*(TWL+TWR)-2.0*PHTWP)/NSUBK
      IF ((TEMPP(I)-GTZ).GT.VPP) GO TO 226
C
C     SET THE CAVITATION FLAG AND DO THE CALCULATIONS ACCOUNTING FOR
C     CAVITATION.
C
      ICAV(I)=1
215   IGT=ICAV(I)
      IAGAIN=0
      GO TO (217,218),IGT
C
C     CAVITY FORMATION.
C
217   PAR1(4)=VCAV(I)
219   TEMPP(I)=VPP+GTZ
      TEMPQ(I)=(TPP1-TEMPP(I)+TQP1*NSUBK-CONST2*TWL-PHTWP)/NSUBK
      QMINUS(I)=(TEMPP(I)-TPM1+TQM1*NSUBK-CONST2*TWR-PHTWP)/
     1 NSUBK
      VCAV(I)=PAR1(4)+0.5*DELTMP*(QMINUS(I)-TEMPQ(I)+QRL(I))
      GO TO (221,222),KIP
221   IF (IAGAIN.EQ.1) GO TO 214
      IF (VCAV(I).LE.0.0) GO TO 214
C
C     AIR RELEASE CONSIDERED.
C
      RVAVL=(VCAV(I)+PAR1(4))*0.5*VOLREF/VL
      VOLAMT=VOLAM*RVAVL/(RVAVL+RKS)
      IF (VOLA(I).GE.VOLAMT) GO TO 214
      VOLA(I)=VOLA(I)+CONST3*(VOLAMT-VOLA(I))
      RM1(I)=VOLA(I)*(VP*14.7)/PF
214   IF (VCAV(I).GE.ALPHI*VOLA(I)) GO TO 225
      IAGAIN=1
      ICAV(I)=2
      GO TO 216
C
```

```
C     NO MORE AIR RELEASE AND BUBBLE FOLLOWS GAS LAW.
C
218   PAR1(4)=VCAV(I)
216   PAR1(1)=1.4
      PAR1(2)=CONST2*TWL+PHTWP
      PAR1(3)=CONST2*TWR+PHTWP
      PAR1(5)=RMI(I)
      PAR1(6)=GTZ+VPP
      PAR1(7)=FLOAT(I)
      PAR1(8)=TQP1
      VCAV(I)=FUNC1(IER)
      IF (IER.EQ.140)  STOP 2160
      IER=0
      IF (TEMPP(I).GE.VPP+GTZ+VPAP) GO TO 225
      IF (IAGAIN.EQ.1) IER=140
      ICAV(I)=1
      IAGAIN=1
      GO TO 219
C
C     VAPOR-ONLY MECHANISM.
C
222   IF (VCAV(I).GT.0.0D0) GO TO 225
      TEMPP(I)=0.5*(TPP1+TPM1+(TQP1-TQM1)*
     1 NSUBK-CONST2*(TWL-TWR))
      TEMPQ(I)=0.5*(TPP1-TPM1+(TQP1+TQM1)*NSUBK
     1 -CONST2*(TWL+TWR)-2.0*PHTWP)/NSUBK
      IF (TEMPP(I)-GTZ.LE.VPP) STOP 222
      VCAV(I)=0.0
      ICAV(I)=0
      ORL(I)=0.0
      GO TO 226
225   ORL(I)=ORINUS(I)-TEMPQ(I)
      IAGAIN=0
226   PA(I)=(TEMPP(1)-GTZ)*PF
 229  CONTINUE
      IREGP=1
      IF (IREG.EQ.2) GO TO 240
      IREG=2
      ASSIGN 222 TO ISKIP
      ITIME=ITIME+1
      POUT=(TEMPP(NGRIDZ)-RG*H(NPSEG))*PF
      QOUT=TEMPQ(NGRIDZ)*QF
      GO TO 259
C
C     LEFT BOUNDARY CALCULATIONS
C
240   TQM1=(1.0-2.0*CRATIO)*TEMPQ(2)+2.0*CRATIO*TEMPQ(1)
      CALL TAUWLV(TQM1,TWR)
      IF (NORFC.LE.1) CALL ORFCO(RSOURC)
      IF (NORFC.LE.2) CALL ORFCO(CS)
      ASSIGN 221 TO ISKIP
      IF  (ORS.LE.0.0) ASSIGN 222 TO ISKIP
      ITIME=ITIME+1
      IF (IFZACT.NE.0) CALL PTAUWE (1,ITIME,NG,CONST2,PHTWP)
      TPM1=(1.0-2.0*CRATIO)*TEMPP(2)+2.0*CRATIO*TEMPP(1)
      IF (ICAV(1).GT.0) GO TO 246
      IF (NORFC.GE.2) GO TO 242
```

```
      TEMPQ(1)=(PINP-TPM1+TQM1*NSUBK-CONST2*TWR
     1 -PHTWP )/(NSUBK+RSOURC)
      TEMPP(1)=PINP-TEMPQ(1)*RSOURC
      GO TO 243
242   C1=-TPM1+TQM1*NSUBK-CONST2*TWR-PHTWP
      CALL QUADC(TEMPP(1),TEMPQ(1),C1,CS,NSUBK,PINP)
C
C     CHECK FOR CAVITATION AND  DO THE NECESSARY CALCULATIONS USING
C     VAPOR-ONLY MECHANISM.
C
243   IF (TEMPP(1).GT.VPP) GO TO 245
      ICAV(1)=1
246   TEMPP(1)=VPP
      IF (NORFC.LE.1) TEMPQ(1)=(PINP-TEMPP(1))/RSOURC
      IF (NORFC.EQ.2) TEMPQ(1)=CS*SIGN(1.0,PINP-TEMPP(1))*SQRT(ABS(
     1 PINP-TEMPP(1)))
      QMINUS(1)=(TEMPP(1)-TPM1+TQM1*NSUBK-CONST2*TWR-PHTWP)/
     1 NSUBK
      VCAV(1)=VCAV(1)+0.5*DELTMP*(QMINUS(1)-TEMPQ(1)+QRL(1))
      QRL(1)=QMINUS(1)-TEMPQ(1)
      IF (VCAV(1).GT.0.0) GO TO 245
      ICAV(1)=0
      VCAV(1)=0.0
      QRL(1)=0.0
      IF (NORFC.GE.2) GO TO 244
      TEMPQ(1)=(PINP-TPM1+TQM1*NSUBK-CONST2*TWR
     1  -PHTWP)/(NSUBK+RSOURC)
      TEMPP(1)=PINP-TEMPQ(1)*RSOURC
      GO TO 2441
244   C1=-TPM1+TQM1*NSUBK-CONST2*TWR-PHTWP
      CALL QUADC(TEMPP(1),TEMPQ(1),C1,CS,NSUBK,PINP)
2441  IF (TEMPP(1).LE.VPP) STOP 4000
C
C     RIGHT BOUNDARY CALCULATIONS
C
245   QPLUS=TEMPQ(NGRIDZ-1)
      PA(1)=TEMPP(1)*PF
      IF (IEZACT.NE.0) CALL PTAUWE (NGRIDZ,ITIME,NG,CONST2,PHTWP)
      IF (ICAV(NGRIDZ-1).GT.0) QPLUS=QMINUS(NGRIDZ-1)
      TOP1=QPLUS*(1.0-2.*CRATIO)+2.*CRATIO*TEMPQ(NGRIDZ)
      CALL TAUWPV(TOP1,TWL)
      TPP1=TEMPP(NGRIDZ-1)*(1.0-2.*CRATIO)+2.*CRATIO*TEMPP(NGRIDZ)
      IF (NORFC.EQ.0) CALL ORFC(RLOAD)
      IF (NORFC.GE.1) CALL ORFC(CL)
      IF (ICAV(NGRIDZ).GT.0) GO TO 248
      IF (NORFC.NE.0) GO TO 2451
      TEMPQ(NGRIDZ)=(TPP1-PLP+TOP1
     1 +NSUBK*CONST2*TWL-PHTWP)/(NSUBK+RLOAD)
      TEMPP(NGRIDZ)=TEMPQ(NGRIDZ)*RLOAD+PEP
      GO TO 2452
2451  C1=TPP1+TOP1*NSUBK-CONST2*TWL-PHTWP
      CALL QUADL(TEMPP(NGRIDZ),TEMPQ(NGRIDZ),C1,CL,NSUBK,PEP)
C
C     CHECK FOR CAVITATION AND DO THE NECESSARY CALCULATIONS USING
C      VAPOR-ONLY MECHANISM.
C
2452  IF ((TEMPP(NGRIDZ)-RG*H(NPSEG)).GT.VPP) GO TO 247
      ICAV(NGRIDZ)=1
```

```
248   TEMPP(NGRIDZ)=VPP+RG*H(NPSEG)
      TEMPQ(NGRIDZ)=(TPP1-TEMPP(NGRIDZ)+TQP1*NSUBK
     1 -CONST2*TWL-PHTWP)/NSUBK
      IF (NORFC.EQ.0) QMINUS(NGRIDZ)=(TEMPP(NGRIDZ)-PEP)/RLOAD
      IF (NORFC.GE.1) QMINUS(NGRIDZ)=CL*SIGN(1.,(TEMPP(NGRIDZ)-PEP))
     1 *SQRT(ABS(TEMPP(NGRIDZ)-PEP))
      VCAV(NGRIDZ)=VCAV(NGRIDZ)+0.5*DELTMP*(QMINUS(NGRIDZ)-TEMPQ(NGRIDZ)
     1 +QRL(NGRIDZ))
      QRL(NGRIDZ)=QMINUS(NGRIDZ)-TEMPQ(NGRIDZ)
      IF (VCAV(NGRIDZ).GT.0.0D0) GO TO 247
      ICAV(NGRIDZ)=0
      VCAV(NGRIDZ)=0.0
      QRL(NGRIDZ)=0.0
      IF (NORFC.NE.0) GO TO 2481
      TEMPQ(NGRIDZ)=(TPP1-PEP+TQP1
     1 *NSUBK-CONST2*TWL-PHTWP)/(NSUBK+RLOAD)
      TEMPP(NGRIDZ)=TEMPQ(NGRIDZ)*RLOAD+PEP
      GO TO 2482
2481  C1=TPP1+TQP1*NSUBK-CONST2*TWL-PHTWP
      CALL QUADL(TEMPP(NGRIDZ),TEMPQ(NGRIDZ),C1,CL,NSUBK,PEP)
2482  IF ((TEMPP(NGRIDZ)-RG*H(NPSEG)).LE.VPP) STOP 5000
247   IBEG=3
      Z=DELTZ
      PA(NGRIDZ)=(TEMPP(NGRIDZ)-RG*H(NPSEG))*PF
      GO TO 260
  250 CONTINUE
      GO TO 1000
  300 CONTINUE
 1000 RETURN
1010  WRITE(6,1020)I
1020  FORMAT(1X/'** ERROR **  Z IS GREATER THAN LINE LENGTH L-- I=',I3/)
1030  FORMAT(1X/'++ WARNING ++   QAPP= ',G11.4/)
      STOP 1010
1040  WRITE (6,1070)
1070  FORMAT(1X,'** ERROR ** CAN NOT HANDLE NORFC=1 AND PIN NE PINIT CAS
     1E'/)
      STOP 1040
      END
C  BLOCK DATA ------------
      BLOCK DATA
      IMPLICIT REAL*8(A-H,O-Z)
      COMMON/NALL/Y(1),DY(1),X(220),P(50),TIME,BEGTIM,
     1           ENDTIM,DELT
      DATA Y,DY,X,P,TIME,BEGTIM,ENDTIM,DELT/1*0.0,
     1    1*0.0,220*0.0,50*0.0,0.0,0.0,0.0,0.0,0.0,0.0/
      END
C   FUNCTION FUNC1 ---------------
      DOUBLE PRECISION FUNCTION FUNC1 (IER1)
C
C     THIS FUNCTION SUBPROGRAM IS USED BY THE SUBROUTINE
C     LINEQ TO SOLVE FOR PRESSURE AND FLOW RATE  AT A GIVEN
C     GRID POINT  WHEN  AIR IS PRESENT IN THE CAVITATION BUBBLE
C     AND FOLLOWS ISOTHERMAL PROCESS.
C
      IMPLICIT REAL*8 (A-H,O-Z)
      COMMON/NALL/Y(1),DY(1),X(220),P(50),TIME,BEGTIM,
     1           ENDTIM,DELT
      COMMON /MISC/PI,NSUBK,MODE
```

```
      COMMON /SOLVER / QRL(101),PAR1(8),
     1 QMINUS(101),DELTMP,CRATIO,TPP1,TPM1,TQM1,ICAV(101)
C
      REAL SNGL
      REAL*8 NSUBK
      COMPLEX*16 ZLG,ZSM,DCMPLX
C
      DIMENSION TEMPP(101),TEMPQ(101),PAR(1)
C
      EQUIVALENCE (P(27),PF)
      EQUIVALENCE (X(11),TEMPP(1)),   (X(112),TEMPQ(1))
C
      I=IFIX(SNGL(PAR1(7))+0.5)
30    RK1=PAR1(6)
      TEMP1=(TPP1+PAR1(8)*NSUBK-PAR1(2))/NSUBK
      TEMP2=(-TPM1+TQM1*NSUBK-PAR1(3))/NSUBK
      RK2=0.5*DELTMP
      TEMP3=RK2*(QRL(I)+TEMP2-TEMP1)+PAR1(4)
      A=1.0
      B=-(TEMP3+2.0*RK2*RK1/NSUBK)
      C=-2.0*RK2*PAR1(5)/NSUBK
      DISC=B*B-4.0*C
      IF (DISC.LT.0.0) ZLG=0.5*DCMPLX(-B,DSQRT(-DISC))
      IF (DISC.GE.0.0) ZLG=(-B+DSQRT(DISC))/2.0
      ZSM=-B-ZLG
      IF (DIMAG(ZLG)/DREAL(ZLG).GT.1.0D-10) GO TO 100
      IF (DREAL(ZLG)*DREAL(ZSM).LT.0.0) GO TO 110
      IER1=129
      WRITE(6,*) ZLG,ZSM,I,TIME,PAR1,QRL(I)
      STOP 129
129   RETURN
110   FUNC1=DMAX1(DREAL(ZSM),DREAL(ZLG))
      RETURN
100   WRITE(6,200) ZLG,ZSM,I,TIME
      IER1=130
200   FORMAT(1X,'COMPLEX ROOTS',6G12.5/)
      RETURN
      END
C
C     FUNCTION SUBPROGRAM F IS USED BY IMSL ROUTINE ZXGSP
C
      FUNCTION F(QP,PAR,PDUM,IDUM,I2,I3)
C
      IMPLICIT REAL*8 (A-H,O-Z)
C
      REAL*8 L
      COMMON /NALL/Y(1),DY(1),X(220),P(50),TIME,BEGTIM,ENDTIM,DELT
      DIMENSION PAR(5),PDUM(1),IDUM(1)
C
      EQUIVALENCE (P(50),NORFC),  (P(12),D)
      ABS(X)=DABS(X)
C
      PD=PAR(1)
      CSOURC=PAR(2)
      CLOAD=PAR(3)
      L=PAR(4)
      CALL TAUWEV(QP,TWP)
      PDL=4.0*L*TWP/D
```

```
IF(NORFC.EQ.0) PDR=QP*(CSOURC+CLOAD)
IF (NORFC.EQ.2) PDR=QP*ABS(QP)*(1./CSOURC**2+1./CLOAD**2)
IF (NORFC.EQ.1) PDR=QP*CSOURC+QP*ABS(QP)/CLOAD**2
F=DABS(PD-PDL-PDR)
RETURN
END
```

VITA

Vijay Kumar Maddali

Candidate for the Degree of

Doctor of Philosophy

Thesis: TRANSIENT RESPONSE OF PIPELINES CARRYING HOMOGENEOUS COAL SLURRIES

Major Field: Mechanical Engineering

Personal Data: Born in Madras, Tamilnadu, India, November 30, 1950, the son of Mr. and Mrs. Venkata Subbayya Maddali.

Education: Graduated from Pfeiffer Memorial High School, Renigunta, Andhra Pradesh, India, in 1966; received Bachelor of Engineering degree in Electronics and Communication Engineering from Andhra University, Waltair, India, in 1972; received the Master of Engineering degree from Indian Institute of Science, Bangalore, India, in 1974; completed the requirements for the Doctor of Philosophy degree at Oklahoma State University in December, 1979.

Professional Experience: Trainee Engineer, National Aeronautics Laboratories, Summer, 1971; Graduate Teaching Assistant and Graduate Research Assistant, 1974 to date.

Professional Organizations: Member of American Society of Mechanical Engineers; Institute of Electrical and Electronic Engineers.